Electronic Supplementary Information

Asymmetric nonfullerene acceptors tuning conformation for efficient organic solar cells†

Linqiang Yang‡, Xin Song‡, Jiangsheng Yu, Hongtao Wang, Zhuohan Zhang, Renyong Geng, Jinru Cao, Derya Baran* and Weihua Tang*

Table of Contents

1. Materials and Synthesis

All commercially available chemicals and solvents were used directly without further purification unless otherwise stated. Tetrahydrofuran (THF) and toluene were distilled before a drying progress of sodium, and 1,2-dichloroethane was dried with calcium hydride. 4-octyl-2-(tributylstannyl)-4H-dithieno[3,2-*b*:2',3'-*d*]pyrrole (compound 1),[1] tributyl(thieno[3,2-*b*]thiophen-2-yl)stannane,[2] and tributyl(dithieno[3,2-*b*:2',3'-*d*]thiophen-2-yl)stannane[3] were synthesized according to the literature.

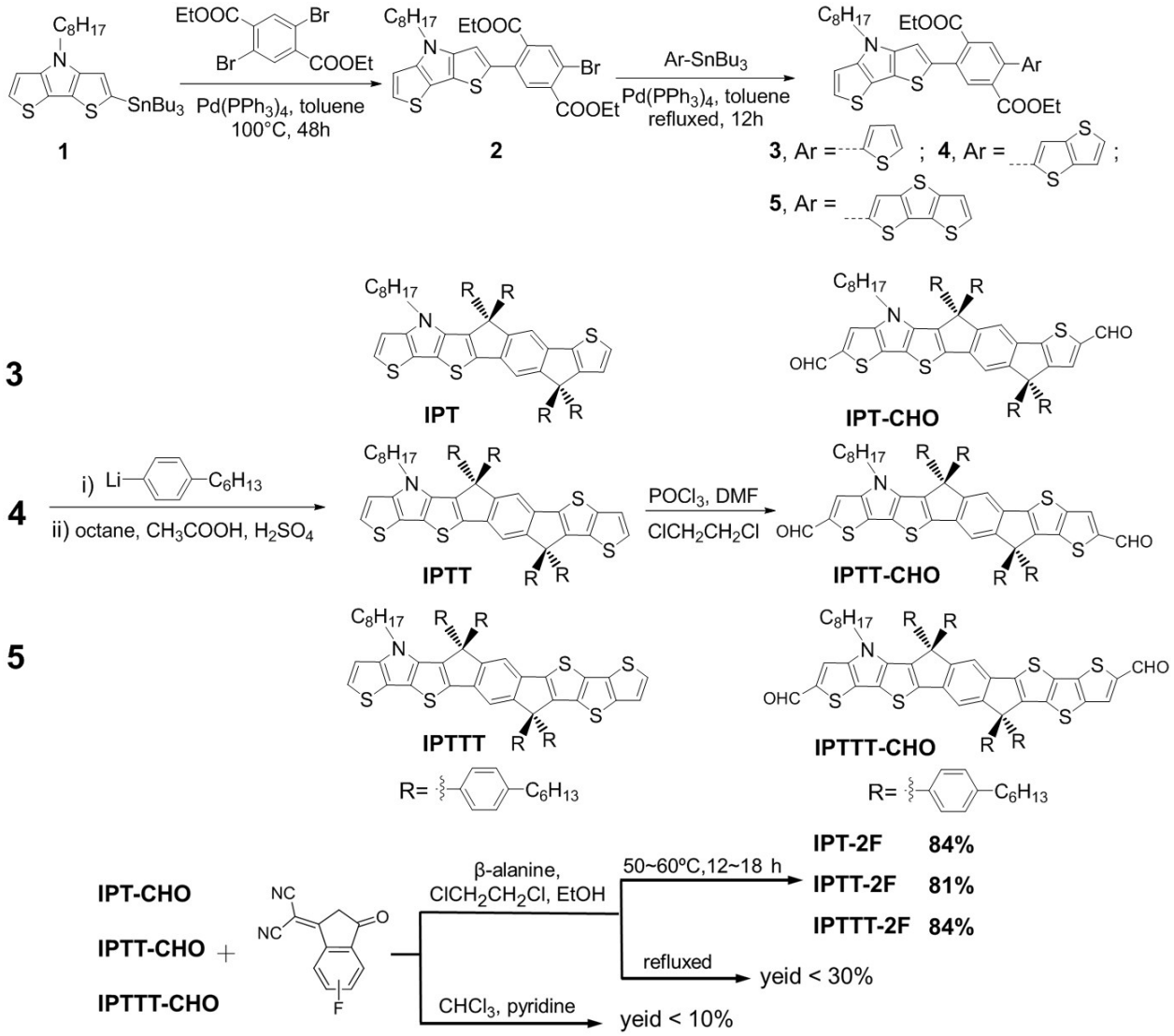

Scheme S1. Synthetic routes of IPT-2F, IPTT-2F, and IPTTT-2F.

Synthesis of diethyl 2-bromo-5-(4-octyl-4H-dithieno[3,2-*b*:2',3'-*d*]pyrrol-2-yl)terephthalate (compound 2): diethyl 2,5-dibromoterephthalate (3.9 g, 10.3 mmol), compound 1 (4.0 g, 6.9 mmol), $Pd(PPh_3)_4$ (159.3 mg, 137.8 μmol) were added in anhydrous toluene (100 mL). The mixture reacted at 100°C for 48 h under nitrogen and then cooled to room temperature. The solvent in the mixture was evaporated under vacuum. The residue was purified by silica gel column chromatography (petroleum ether/ethyl acetate=15:1 v/v) to obtain an orange viscous liquid (2.2 g, 54%). ^{1}H NMR (500 MHz, $CDCl_3$, δ): 7.95 (d, *J* = 1.9 Hz, 2H), 7.17 (d, *J* = 5.3 Hz, 1H), 7.04 (s, 1H), 7.00 (d, *J* = 5.3 Hz, 1H), 4.44 (m, 2H), 4.24 (m, 2H), 4.18 (t, *J* = 7.0 Hz, 2H), 1.86 (m, 2H), 1.42 (t, *J* = 7.1 Hz, 3H), 1.35 - 1.19 (m, 10H), 1.16 (t, *J* = 7.1 Hz, 3H), 0.86 (t, *J* = 6.9 Hz, 3H). ^{13}C NMR (125 MHz, $CDCl_3$, δ): 167.20, 165.47, 145.01, 144.71, 136.49, 135.36, 134.85, 134.50, 134.15, 133.42, 123.95, 120.18, 116.02, 114.84, 111.27, 111.06, 62.25, 62.08, 47.61, 31.92, 30.53, 29.38, 29.27, 27.15, 22.75, 14.35, 14.22, 14.07. MALDI-TOF MS (*m*/*z*): $[M+H]^+$ calcd. for $C_{28}H_{32}BrNO_4S_2$, 589.0956; found, 589.0952.

Synthesis of diethyl 2-(4-octyl-4H-dithieno[3,2-*b*:2',3'-*d*]pyrrol-2-yl)-5-(thiophen-2-yl)terephthalate (compound 3): Compound 2 (570.0 mg, 1.0 mmol), tributyl(thiophen-2-yl)stannane (468.2 mg, 1.3 mmol), $Pd(PPh_3)_4$ (55.8 mg, 48.3 μmol) were added in anhydrous toluene (12 mL). The mixture was refluxed for 12 h under nitrogen. The solvent in the mixture was evaporated under

vacuum. The residue was purified by silica gel column chromatography (petroleum ether/dichloromethane=3:2 v/v) to obtain an orange viscous liquid (460 mg, 80%). ^{1}H NMR (500 MHz, $CDCl_3$, δ): 7.93 (s, 1H), 7.80 (s, 1H), 7.40 (d, *J* = 3.8 Hz, 1H), 7.17 (d, *J* = 5.3 Hz, 1H), 7.12 (d, *J* = 2.3 Hz, 1H), 7.09 (m, 2H), 7.02 (d, *J* = 5.3 Hz, 1H), 4.29 - 4.18 (m, 6H), 1.88 (m, 2H), 1.37 - 1.22 (m, 10H), 1.17 (m, 6H), 0.88 (t, *J* = 6.9 Hz, 3H). ^{13}C NMR (125 MHz, $CDCl_3$, δ): 168.36, 167.93, 144.95, 144.78, 140.71, 137.29, 134.26, 134.11, 134.09, 133.04, 131.80, 131.76, 127.49, 127.05, 126.56, 123.80, 115.98, 114.86, 111.10, 111.04, 61.87, 61.78, 47.59, 31.92, 30.53, 29.39, 29.27, 27.15, 22.74, 14.23, 14.09, 13.95. MALDI-TOF MS (*m*/*z*): $[M+H]^+$ calcd. for $C_{32}H_{35}NO_4S_3$, 593.1728; found, 593.1724.

Synthesis of diethyl 2-(4-octyl-4H-dithieno[3,2-*b*:2',3'-*d*]pyrrol-2-yl)-5-(thieno[3,2-b]thiophen-2-yl)terephthalate (compound 4): Compound 2 (500 mg, 0.9 mmol), tributyl(thieno[3,2-b]thiophen-2-yl)stannane (472.5 mg, 1.1 mmol), $Pd(PPh_3)_4$ (48.9 mg, 42.3 μmol) were added in anhydrous toluene (12 mL). The mixture was refluxed for 12 h under nitrogen. The solvent in the mixture was evaporated under vacuum. The residue was purified by silica gel column chromatography (petroleum ether/dichloromethane=3:2 v/v) to obtain an orange viscous liquid (450 mg, 81%). ^{1}H NMR (500 MHz, $CDCl_3$, δ): 7.95 (s, 1H), 7.85 (s, 1H), 7.40 (d, *J* = 5.2 Hz, 1H), 7.33 - 7.29 (m, 2H), 7.18 (d, *J* = 5.3 Hz, 1H), 7.10 (s, 1H), 7.02 (d, *J* = 5.3 Hz, 1H), 4.28 (m, 4H), 4.20 (t, *J* = 7.0 Hz, 2H), 1.88 (m, 2H), 1.36 - 1.22 (m, 10H), 1.17 (m, 6H), 0.87 (t, *J* = 6.8 Hz, 3H). ^{13}C NMR (125 MHz, $CDCl_3$, δ): 168.31, 167.80, 145.02, 144.82, 142.40, 139.97, 139.51, 137.19, 134.58, 134.16, 134.06, 133.10, 131.90, 131.89, 127.44, 123.91, 119.57, 119.31, 116.10, 114.89, 111.20, 111.06, 61.95, 61.92, 47.63, 31.94, 30.55, 29.41, 29.30, 27.18, 22.76, 14.25, 14.11, 14.00. MALDI-TOF MS (*m*/*z*): $[M+H]^+$ calcd. for $C_{34}H_{35}NO_4S_4$, 649.1449; found, 649.1444.

Synthesis of diethyl 2-(dithieno[3,2-*b*:2',3'-*d*]thiophen-2-yl)-5-(4-octyl-4H-dithieno[3,2-*b*:2',3'-*d*]pyrrol-2-yl)terephthalate (compound 5): Compound 2 (500 mg, 0.9 mmol), tributyl(dithieno[3,2-*b*:2',3'-*d*]thiophen-2-yl)stannane (534.2 mg, 1.1 mmol), $Pd(PPh_3)_4$ (48.9 mg, 42.3 μmol) were added in anhydrous toluene (12 mL). The mixture was refluxed for 12 h under nitrogen. The solvent in the mixture was evaporated under vacuum. The residue was purified by silica gel column chromatography (petroleum ether/dichloromethane=1:1 v/v) to obtain a yellow solid (500 mg, 84%). ^{1}H NMR (500 MHz, $CDCl_3$, δ): 7.94 (s, 1H), 7.84 (s, 1H), 7.40 (d, *J* = 5.2 Hz, 1H), 7.30 (s, 1H), 7.28 (d, *J* = 5.2 Hz, 1H), 7.18 (d, *J* = 5.3 Hz, 1H), 7.10 (s, 1H), 7.02 (d, *J* = 5.3 Hz, 1H), 4.27 (m, 4H), 4.20 (t, *J* = 7.1 Hz, 2H), 1.88 (m, 2H), 1.35 - 1.23 (m, 10H), 1.16 (m, 6H), 0.88 (t, *J* = 6.8 Hz, 3H). ^{13}C NMR (125 MHz, $CDCl_3$, δ): 168.31, 167.78, 145.08, 144.86, 141.64, 141.54, 140.96, 137.17, 134.69, 134.25, 134.01, 132.79, 132.02, 131.93, 131.62, 131.04, 126.55, 123.97, 120.94, 120.73, 116.18, 114.93, 111.26, 111.09, 62.01, 47.67, 31.97, 30.59, 29.44, 29.33, 27.21, 22.79, 14.27, 14.15, 14.10. MALDI-TOF MS (*m*/*z*): $[M+H]^+$ calcd. for $C_{36}H_{35}NO_4S_5$, 705.1170; found, 705.1165.

Synthesis of IPT: A solution of 4-hexyl-1-bromobenzene (1.3 g, 5.2 mmol) in anhydrous THF (30 mL) was placed at -78°C for 10 min, then *n*-BuLi (1.9 mL, 4.8 mmol, 2.5 M in hexane) was added to the solution slowly. After the mixture was stirred for 2 h at -78°C under nitrogen, compound **3** (410.0 mg, 0.7 mmol) in THF (5 mL) was then added to the solution in a minute. The reaction mixture was warmed to room temperature and stirred for 2 h. The solvent of the mixture was evaporated under vacuum. The light yellow residue was dissolved in octane (80 mL) and acetic acid (40 mL), then 0.1 mL concentrated H_2SO_4 was added dropwise. The solution was stirred at room temperature for 1 h before quenched by water. The organic layer was extracted with petroleum ether (2×100 mL) and washed with water for three times. The combined organic phase was dried over anhydrous $MgSO_4$. The solvent in the mixture was evaporated under vacuum, and the residue was purified by silica gel column chromatography (petroleum ether/dichloromethane=9:1 v/v) to obtain a viscous yellow liquid (700 mg, 91%). ^{1}H NMR (500 MHz, CD_2Cl_2, δ): 7.50 (s, 1H), 7.44 (s, 1H), 7.38 (d, *J* = 8.1 Hz, 4H), 7.28 (d, *J* = 4.9 Hz, 1H), 7.18 (d, *J* = 8.1 Hz, 4H), 7.17 - 7.10 (m, 10H), 7.01 (d, *J* = 4.9 Hz, 1H), 6.95 (d, *J* = 5.2 Hz, 1H), 3.81 - 3.74 (m, 2H), 2.59 (m, 8H), 1.64 - 1.57 (m, 8H), 1.39 - 1.28 (m, 28H), 1.25 - 1.15 (m, 4H), 1.12 - 1.02 (m, 4H), 0.92 - 0.88 (m, 15H). ^{13}C NMR (125 MHz, CD_2Cl_2, δ): 156.79, 156.09, 153.92, 145.00, 142.44, 142.41, 142.07, 141.61, 140.69, 140.36, 139.88, 138.93, 136.19, 135.24, 129.06, 128.81, 128.78, 128.17, 127.88, 123.39, 123.29, 118.09, 116.43, 116.40, 116.28, 111.98, 63.10, 62.90, 48.70, 35.91, 32.34, 32.16, 31.91, 31.84, 30.76, 29.76, 29.71, 29.58, 29.56, 27.22, 23.11, 23.05, 14.34, 14.32. MALDI-TOF MS (*m*/*z*): $[M+H]^+$ calcd. for $C_{76}H_{91}NS_3$, 1113.6314; found, 1113.6307.

Synthesis of IPTT: The synthetic method of compound IPTT was similar to the synthesis of compound IPT. The residue was purified by silica gel column chromatography (petroleum ether/dichloromethane=9:1 v/v) to obtain a yellow solid (92%). ^{1}H NMR (500 MHz, CD_2Cl_2, δ): 7.53 (s, 1H), 7.51 (s, 1H), 7.41 (d, *J* = 8.1 Hz, 4H), 7.30 (m, 2H), 7.21 (d, *J* = 8.1 Hz, 4H), 7.17 - 7.11 (m, 9H), 6.95 (d, *J* = 5.2 Hz, 1H), 3.82 - 3.74 (m, 2H), 2.60 (m, 8H), 1.61 (m, 8H), 1.39 - 1.29 (m, 28H), 1.21 (m, 4H), 1.07 (m, 4H), 0.93 - 0.89 (m, 15H). ^{13}C NMR (125 MHz, CD_2Cl_2, δ): 156.99, 153.59, 146.09, 145.07, 143.70, 142.49, 142.43, 142.07, 140.82, 140.67, 140.30, 139.86, 138.85, 136.57, 135.85, 133.99, 129.08, 128.92, 128.85, 128.36, 126.76, 123.39, 120.90, 118.24, 116.42, 116.21, 115.95, 111.99, 63.37, 62.94, 48.71, 35.95, 35.92, 32.35, 32.16, 32.15, 31.85, 31.85, 30.77, 29.77, 29.72, 29.60, 27.24, 23.12, 23.06, 23.04, 14.35, 14.32. MALDI-TOF MS (*m*/*z*): $[M+H]^+$ calcd. for $C_{78}H_{91}NS_4$, 1169.6034; found, 1169.6204.

Synthesis of IPTTT: The synthetic method of compound IPTTT was similar to the synthesis of compound IPT. The residue was purified by silica gel column chromatography (petroleum ether/dichloromethane=9:1 v/v) to obtain a yellow solid (90%). ^{1}H NMR (500 MHz, CD_2Cl_2, δ): 7.55 (s, 1H), 7.52 (s, 1H), 7.42 (d, *J* = 8.2 Hz, 4H), 7.31 (d, *J* = 5.2 Hz, 1H), 7.25 - 7.21 (m, 5H), 7.18 - 7.11 (m, 9H), 6.95 (d, *J* = 5.3 Hz, 1H), 3.82 - 3.74 (m, 2H), 2.60 (m, 8H), 1.65 - 1.57 (m, 8H), 1.33 (m, 28H), 1.27 - 1.18 (m, 4H), 1.08 (m, 4H), 0.94 - 0.88 (m, 15H). ^{13}C NMR (125 MHz, CD_2Cl_2, δ): 157.08, 153.74, 147.41, 145.13, 142.53, 142.42, 141.64, 140.90, 140.43, 140.28, 139.88, 138.84, 136.70, 136.34, 135.60, 132.91, 132.12, 129.11, 128.96, 128.88, 128.43, 126.07, 123.45, 121.08, 118.33, 116.45, 116.12, 115.91, 112.00, 63.51, 62.99, 48.73, 35.96, 35.93, 32.36, 32.17, 32.15, 31.85, 30.78, 29.78, 29.72, 29.60, 29.59, 27.25, 23.13, 23.06, 23.04, 14.36, 14.32. MALDI-TOF MS (*m*/*z*): $[M+H]^+$ calcd. for $C_{80}H_{91}NS_5$, 1225.5755; found, 1225.5926.

Synthesis of IPT-CHO: A mixed solution of compound IPT (600.0 mg, 538.2 μmol) in anhydrous DMF (4 mL) and anhydrous 1,2-dichloroethane (12 mL) was placed at 0°C for 10 min, then phosphorus oxychloride ($POCl_3$, 0.5 mL) was slowly added to the solution under nitrogen. After being stirred at 0°C for several minutes, the mixture was warmed to 70°C for 3 h. The reaction mixture was poured into a solution of Na_2CO_3 (21.2 g, 0.2 mol) in water (200 mL). The mixture was vigorously stirred at room temperature for 6 h. The organics were extracted with a mixed solvent of ethyl acetate and petroleum ether (1:9, v/v). The combined organic layer was washed with water and dried with anhydrous Mg_2SO_4. The solvent was evaporated under vacuum, and the residue was purified by silica gel column chromatography (petroleum ether/dichloromethane=1:1 v/v) to obtain an orange solid (570 mg, 90%). ^{1}H NMR (500 MHz, CD_2Cl_2, δ): 9.85 (s, 1H), 9.81 (s, 1H), 7.67 (s, 2H), 7.59 (s, 1H), 7.54 (s, 1H), 7.37 (d, *J* = 8.0 Hz, 4H), 7.19 - 7.10 (m, 12H), 3.82 (t, *J* = 8.1 Hz, 2H), 2.59 (m, 8H), 1.63 - 1.56 (m, 8H), 1.41 - 1.27 (m, 28H), 1.24 - 1.03 (m, 8H), 0.92 - 0.87 (m, 15H). ^{13}C NMR (125 MHz, CD_2Cl_2, δ): 183.05, 183.02, 157.77, 156.68, 155.39, 151.00, 146.27, 145.30, 144.59, 143.91, 142.91, 142.60, 141.29, 140.95, 140.75, 137.99, 137.90, 134.72, 132.35, 129.02, 128.97, 128.06, 124.30, 120.46, 119.10, 118.17, 117.15, 63.37, 63.08, 48.83, 35.88, 32.30, 32.13, 31.85, 31.78, 30.81, 29.73, 29.67, 29.55, 29.51, 27.19, 23.09, 23.03, 14.32, 14.30. MALDI-TOF MS (*m*/*z*): $[M+H]^+$ calcd. for $C_{78}H_{91}NO_2S_3$, 1169.6212; found, 1169.6205.

Synthesis of IPTT-CHO: The synthetic method of compound IPTT-CHO was similar to the synthesis of compound IPT-CHO. The residue was purified by silica gel column chromatography (petroleum ether/dichloromethane=1:1 v/v) to obtain an orange solid (88%). ^{1}H NMR (500 MHz, CD_2Cl_2, δ): 9.86 (s, 1H), 9.85 (s, 1H), 7.95 (s, 1H), 7.65 - 7.58 (m, 3H), 7.39 (d, *J* = 7.9 Hz, 4H), 7.19 - 7.12 (m, 12H), 3.83 (t, *J* = 8.1 Hz, 2H), 2.59 (m, 8H), 1.60 (m, 8H), 1.38 - 1.28 (m, 28H), 1.26 - 1.18 (m, 4H), 1.10 (m, 4H), 0.90 (m, 15H). ^{13}C NMR (125 MHz, CD_2Cl_2, δ): 183.10, 182.97, 157.79, 154.82, 150.17, 146.47, 145.50, 144.59, 144.50, 143.96, 142.88, 142.83, 142.11, 140.61, 140.19, 139.77, 138.10, 137.23, 135.99, 130.46, 129.13, 129.02, 128.99, 128.21, 124.36, 120.45, 118.90, 117.34, 116.88, 63.48, 63.08, 48.82, 35.91, 35.89, 32.31, 32.12, 32.11, 31.80, 30.82, 29.73, 29.68, 29.56, 29.54, 27.20, 23.09, 23.03, 23.01, 14.33, 14.30. MALDI-TOF MS (*m*/*z*): $[M+H]^+$ calcd. for $C_{80}H_{91}NO_2S_4$, 1225.5933; found, 1225.5928.

Synthesis of IPTTT-CHO: The synthetic method of compound IPTTT-CHO was similar to the synthesis of compound IPT-CHO. The residue was purified by silica gel column chromatography (petroleum ether/dichloromethane=2:3 v/v) to obtain an orange solid (87%). ^{1}H NMR (500 MHz, CD_2Cl_2, δ): 9.85 (d, 2H), 7.79 (s, 1H), 7.63 - 7.57 (m, 3H), 7.39 (d, *J* = 8.1 Hz, 4H), 7.21 (d, *J* = 8.1 Hz, 4H), 7.17 (d, *J* = 8.1 Hz, 4H), 7.13 (d, *J* = 8.1 Hz, 4H), 3.83 (t, *J* = 8.1 Hz, 2H), 2.59 (m, 8H), 1.64 - 1.55 (m, 8H), 1.38 - 1.27 (m, 28H), 1.21 (m, 4H), 1.15 - 1.03 (m, 4H), 0.90 (m, 15H). ^{13}C NMR (125 MHz, CD_2Cl_2, δ): 182.99, 182.96, 157.80, 154.39, 147.72, 146.17, 145.60, 144.44, 144.01, 143.68, 142.87, 142.83, 141.43, 140.78, 140.52, 140.43, 139.81, 138.76, 138.13, 136.76, 136.15, 133.02, 130.56, 129.08, 129.01, 128.99, 128.31, 124.39, 120.43, 118.73, 116.89, 116.77, 63.57, 63.10, 48.81, 35.91, 35.88, 32.30, 32.12, 32.10, 31.81, 31.79, 30.82, 29.73, 29.68, 29.56, 29.53, 27.20, 23.09, 23.03, 23.01, 14.33, 14.29. MALDI-TOF MS (*m*/*z*): $[M+H]^+$ calcd. for $C_{82}H_{91}NO_2S_5$, 1281.5653; found, 1281.5647.

Synthesis of IPT-2F: Compound IPT-CHO (130.0 mg, 111.0 μmol), 2-(5/6-fluoro-3-oxo-2,3-dihydro-1H-inden-1-ylidene) malononitrile (117.8 mg, 555.2 μmol) and β-alanine (2.0 mg, 22.2 μmol) were dissolved in a mixed solvent of 1,2-dichloroethane (8 mL) and EtOH (3 mL). The mixture was placed at 60°C for several hours and the reaction process was monitored by TLC. The solvent in the mixture was evaporated under vacuum. The residue was purified by silica gel column chromatography (petroleum ether/dichloromethane=3:2 v/v) to obtain a dark-blue solid (146 mg, 84%). ^{1}H NMR (500 MHz, $CDCl_3$, δ): 8.86 (m, 2H), 8.70 - 8.60 (m, 0.5H), 8.37 - 8.30 (m, 1.5H), 7.90 - 7.82 (m, 1.5H), 7.69 - 7.67 (m, 2H), 7.58 - 7.47 (m, 2.5H), 7.39 (m, 1H), 7.33 - 7.30 (m, 5H), 7.16 - 7.11 (m, 12H), 3.78 (t, *J* = 8.1 Hz, 2H), 2.59 (m, 8H), 1.60 (m, 8H), 1.38 - 1.26 (m, 28H), 1.24 - 1.15 (m, 4H), 1.12 - 0.99 (m, 4H), 0.88 (m, 15H). ^{13}C NMR (125 MHz, $CDCl_3$, δ): 187.16, 187.05, 167.90, 165.85, 165.65, 160.70, 159.49, 159.47, 159.45, 159.17, 159.16, 159.14, 158.53, 157.82, 157.79, 156.54, 150.43, 150.40, 147.27, 147.23, 146.71, 142.87, 142.54, 142.51, 142.47, 142.39, 140.91, 140.87, 140.66, 140.55, 140.03, 140.00, 138.78, 138.73, 138.58, 137.21, 136.62, 135.99, 135.55, 135.51, 134.72, 133.28, 133.16, 133.15, 128.94, 128.92, 128.66, 127.92, 126.09, 126.01, 125.94, 125.61, 125.54, 121.97, 121.77, 121.74, 121.67, 121.35, 121.15, 120.34, 120.29, 118.92, 118.91, 117.65, 115.46, 115.33, 115.04, 114.57, 114.48, 113.07, 112.86, 112.83, 112.62, 69.73, 67.62, 67.61, 63.12, 62.78, 62.77, 48.73, 35.76, 35.73, 32.07, 31.90, 31.88, 31.51, 31.46, 30.64, 29.54, 29.44, 29.35, 29.30, 26.98, 22.86, 22.79, 14.31, 14.29. ^{19}F NMR (470 MHz, $CDCl_3$, δ): -99.01, -99.02, -99.04, -99.05, -100.08, -100.10, -100.11, -100.13, -100.35, -101.31. MALDI-TOF MS (*m*/*z*): $[M+H]^+$ calcd. for $C_{102}H_{97}F_2N_5O_2S_3$, 1557.6772; found, 1557.6766.

Synthesis of IPTT-2F: By utilizing the similar synthetic method as used for IPT-2F, compound IPTT-CHO (130.0 mg, 106.0 μmol) and 2-(5/6-fluoro-3-oxo-2,3-dihydro-1H-inden-1-ylidene) malononitrile (112.4 mg, 529.8 μmol) and β-alanine (1.9 mg, 21.2 μmol) were used for the synthesis of IPTT-2F. The target compound was obtained as a dark-blue solid (140 mg, 81%). ^{1}H NMR (500 MHz, $CDCl_3$, δ): 8.84 (m, 2H), 8.69 - 8.60 (m, 0.5H), 8.35 - 8.29 (m, 1.5H), 8.20 - 8.18 (m, 1H), 7.91 - 7.81 (m, 1.5H), 7.62 - 7.46 (m, 3.5H), 7.41 - 7.27 (m, 6H), 7.21 (d, *J* = 8.5 Hz, 4H), 7.16 - 7.14 (m, 8H), 3.80 - 3.74 (m, 2H), 2.58 (m, 8H), 1.63 - 1.57 (m, 8H), 1.37 - 1.26 (m, 28H), 1.23 - 1.15 (m, 4H), 1.13 - 0.99 (m, 4H), 0.90 - 0.85 (m, 15H). ^{13}C NMR (125 MHz, $CDCl_3$, δ): 187.06, 186.95, 186.85, 167.88, 167.68, 167.29, 165.83, 165.64, 165.41, 165.23, 159.97, 159.48, 159.13, 159.11, 158.27, 155.73, 153.94, 153.89, 150.79, 147.89, 147.73, 147.45, 147.41, 146.65, 143.71, 142.85, 142.66, 142.54, 142.46, 140.12, 139.54, 139.52, 139.15, 138.66, 138.55, 138.46, 137.46, 137.42, 137.37, 136.56, 136.45, 136.07, 135.99, 135.97, 134.97, 134.78, 133.25, 133.24, 133.15, 133.14, 129.04, 129.04, 128.91, 128.71, 128.08, 126.07, 125.99, 125.57, 125.49, 124.61, 122.47, 122.38, 122.02, 121.83, 121.69, 121.51, 121.28, 121.09, 120.22, 120.19, 120.13, 119.98, 119.94, 119.84, 117.74, 117.42, 115.53, 115.40, 115.11, 114.52, 114.44, 113.02, 112.81, 112.59, 70.04, 67.38, 63.35, 62.89, 48.71, 35.80, 35.73, 32.08, 31.90, 31.88, 31.45, 31.43, 29.55, 29.45, 29.38, 29.37, 27.00, 22.86, 22.79, 14.31, 14.28. ^{19}F NMR (470 MHz, $CDCl_3$, δ): -98.88, -98.90, -98.91, -100.18, -100.24, -100.25, -101.45. MALDI-TOF MS (*m*/*z*): $[M+H]^+$ calcd. for $C_{104}H_{97}F_2N_5O_2S_4$, 1613.6493; found, 1613.6489.

Synthesis of IPTTT-2F: By utilizing the similar synthetic method as used for IPT-2F, compound IPTTT-CHO (130.0 mg, 101.3 μmol) and 2-(5/6-fluoro-3-oxo-2,3-dihydro-1H-inden-1-ylidene)malononitrile (107.5 mg, 506.7 μmol) and β-alanine (1.8 mg, 20.3 μmol) were used for the synthesis of IPTTT-2F. The target compound was obtained as a dark-blue solid (143 mg, 84%). ^{1}H NMR (500 MHz, $CDCl_3$, δ): 8.90 - 8.79 (m, 2H), 8.56 - 8.62 (m, 0.5H), 8.32 - 8.25 (m, 1.5H), 7.90 - 7.77 (m, 3H), 7.57 (s, 2H), 7.52 - 7.44 (m, 1H), 7.36 (d, *J* = 8.2 Hz, 4H), 7.32 - 7.27 (m, 1.5H), 7.24 (m, 0.5H), 7.19 - 7.15 (m, 8H), 7.13 (d, *J* = 8.2 Hz, 4H), 3.77 (t, *J* = 8.2 Hz, 2H), 2.59 (m, 8H), 1.66 - 1.56 (m, 8H), 1.37 - 1.26 (m, 28H), 1.24 - 1.17 (m, 4H), 1.13 - 1.03 (m, 4H), 0.88 (m, 15H). ^{13}C NMR (125 MHz, $CDCl_3$, δ): 187.15, 187.06, 186.94, 167.90, 167.63, 165.85, 165.59, 159.45, 158.82, 158.30, 154.84, 151.15, 149.03, 149.00, 148.32, 147.63, 147.60, 146.61, 143.47, 143.43, 142.98, 142.95, 142.82, 142.69, 142.54, 142.46, 139.79, 139.19, 138.44, 138.28, 138.12, 138.08, 137.65, 137.51, 136.94, 136.69, 136.33, 133.23, 133.19, 133.15, 133.11, 133.09, 133.09, 128.97, 128.92, 128.75, 128.10, 126.07, 125.99, 125.48, 125.40, 122.16, 122.09, 121.94, 121.75, 121.16, 120.98, 119.97, 119.74, 119.69, 117.31, 117.17, 115.57, 115.45, 115.15, 114.53, 114.37, 112.75, 112.54, 70.17, 67.20, 63.37, 62.93, 48.71, 35.79, 35.75, 32.09, 31.89, 31.46, 31.43, 30.62, 29.56, 29.46, 29.38, 29.34, 27.01, 22.87, 22.80, 22.78, 14.32, 14.28. ^{19}F NMR (470 MHz, $CDCl_3$, δ): -98.65, -98.66, -98.67, -100.12, -100.30, -100.32, -100.33, -101.55. MALDI-TOF MS (*m*/*z*): $[M+H]^+$ calcd. for $C_{106}H_{97}F_2N_5O_2S_5$, 1669.6214; found, 1669.6209.

2. Materials Characterization

^{1}H, ^{13}C, and ^{19}F NMR spectra were obtained on a Bruker AVANCE III 500 MHz instrument with solutions in either $CDCl_3$ or CD_2Cl_2. The matrix-assisted laser desorption/ionization time-of-flight (MALDI-TOF) mass spectra were measured by a Bruker Autoflex TOF/TOF spectrometer. Ultraviolet-visible (UV-Vis) absorption spectra were performed on Thermo Fisher Evolution 220. The thermogravimetric analysis (TGA) was tested on NETZSCH TG 209F1 Libra with a heating rate of 20°C min^{-1} from 40 to 800°C under nitrogen gas flow. Differential scanning calorimeter (DSC) analysis was carried out on PerkinElmer Diamond DSC with a heating rate of 40°C min^{-1} from 30 to 250°C in nitrogen atmosphere. The DSC tests were conducted with two cycles of heating and cooling, with the final data collected from the second cycle. Cyclic voltammetry measurements were carried out on CHI 600D electrochemical workstation. All initial potentials were determined in a 0.1 M Bu_4NPF_6 acetonitrile solution under N_2 atmosphere at a scan rate of 50 mV s^{-1} and corrected against ferrocene/ferrocenium (Fc/Fc^+).

3. NMR and Mass Spectra

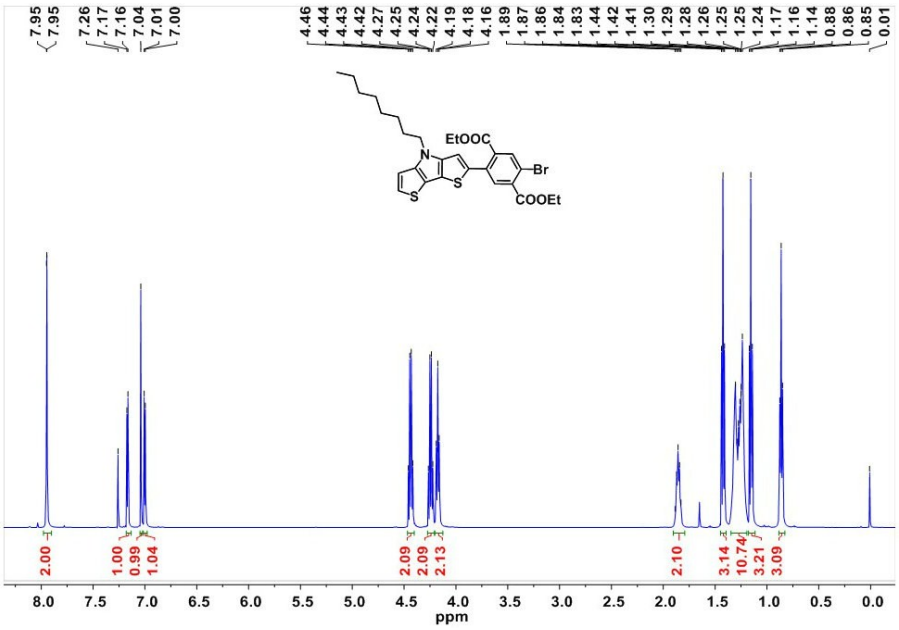

Fig. S1 ^{1}H NMR spectrum of compund 2.

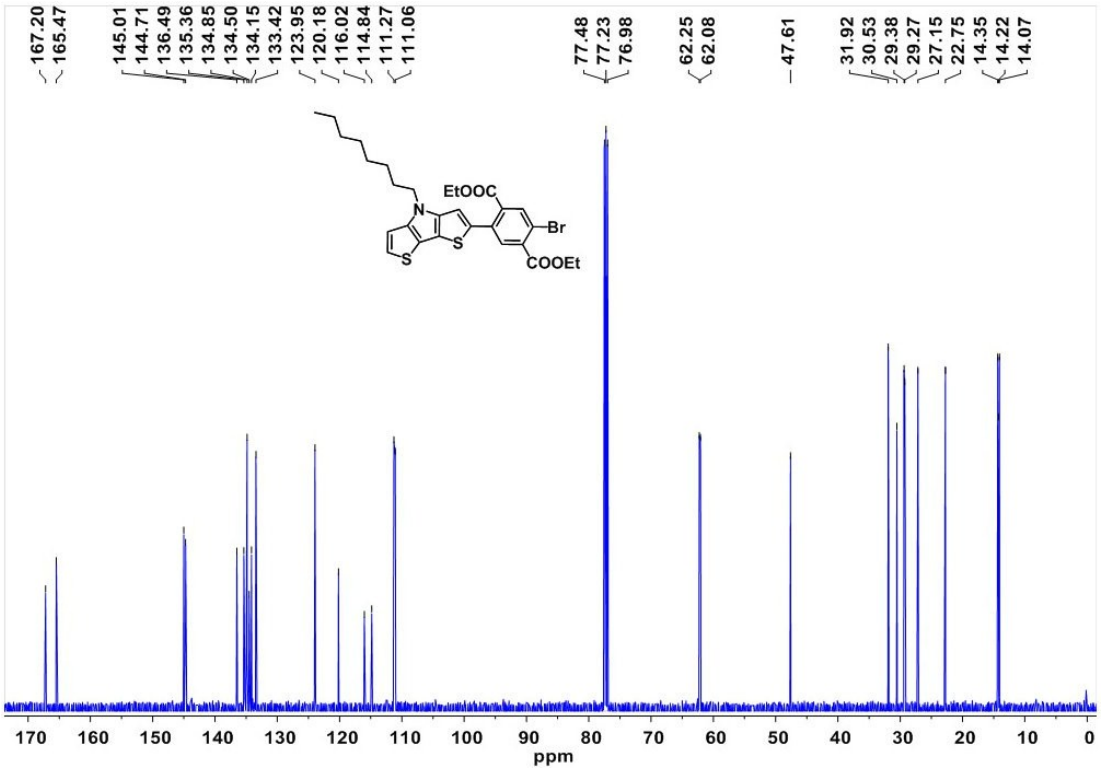

Fig. S2 ^{13}C NMR spectrum of compund 2.

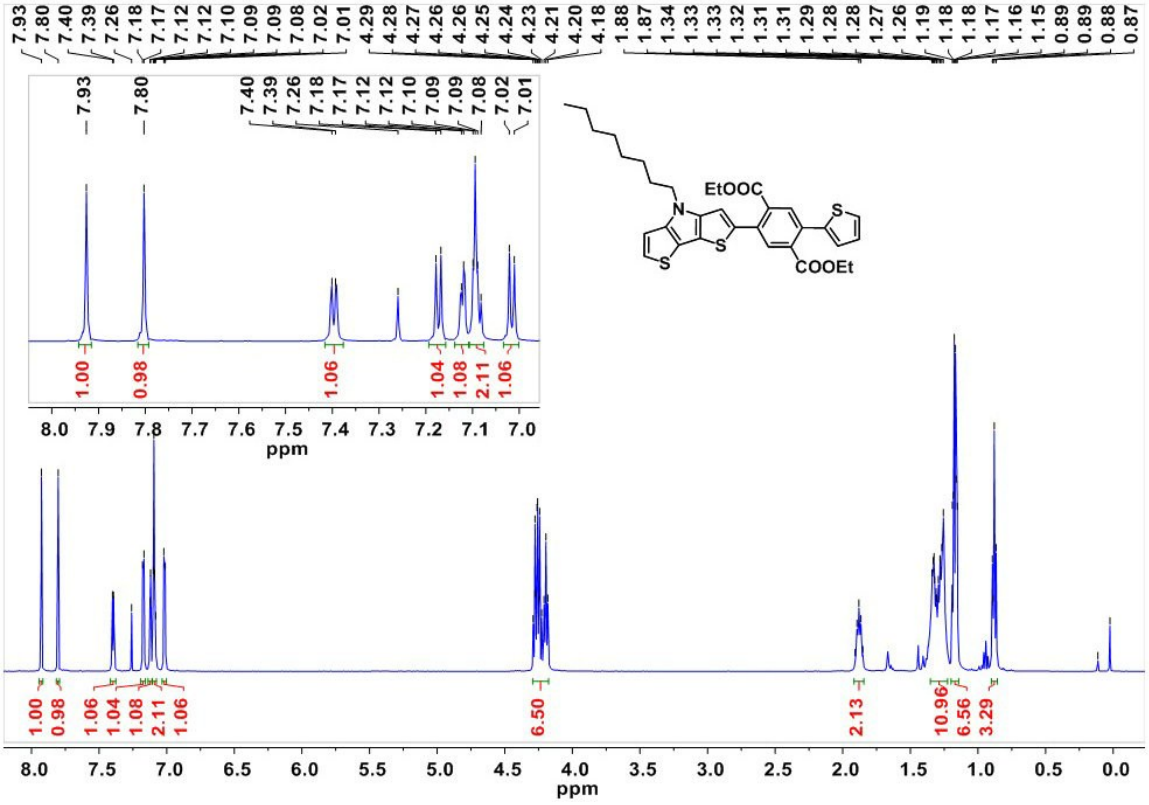

Fig. S3 ^{1}H NMR spectrum of compund 3.

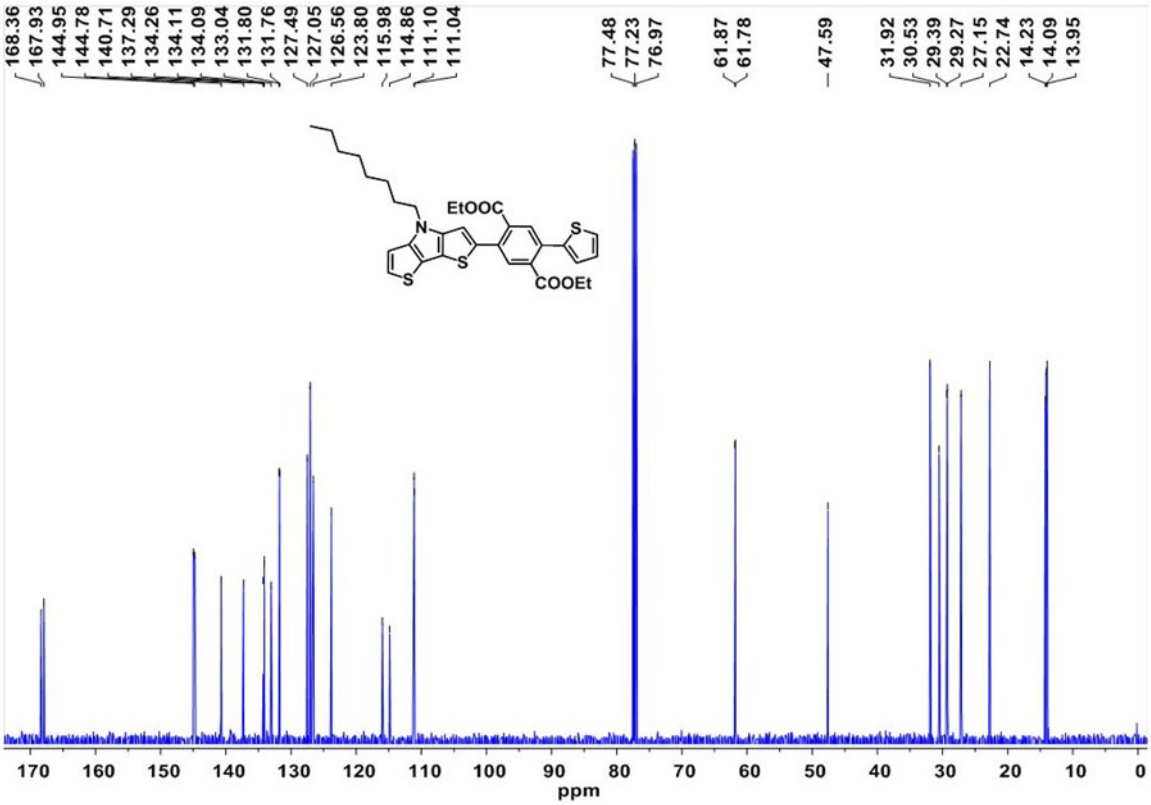

Fig. S4 ^{13}C NMR spectrum of compund 3.

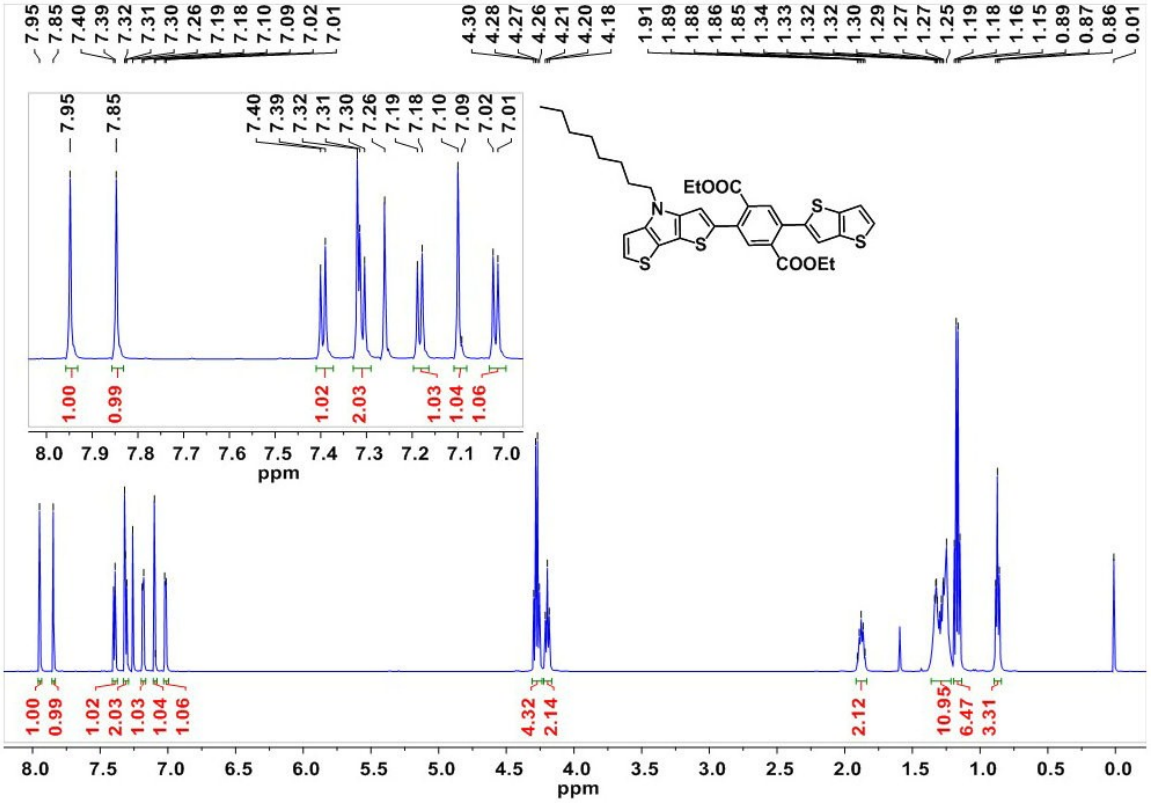

Fig. S5 ^{1}H NMR spectrum of compund 4.

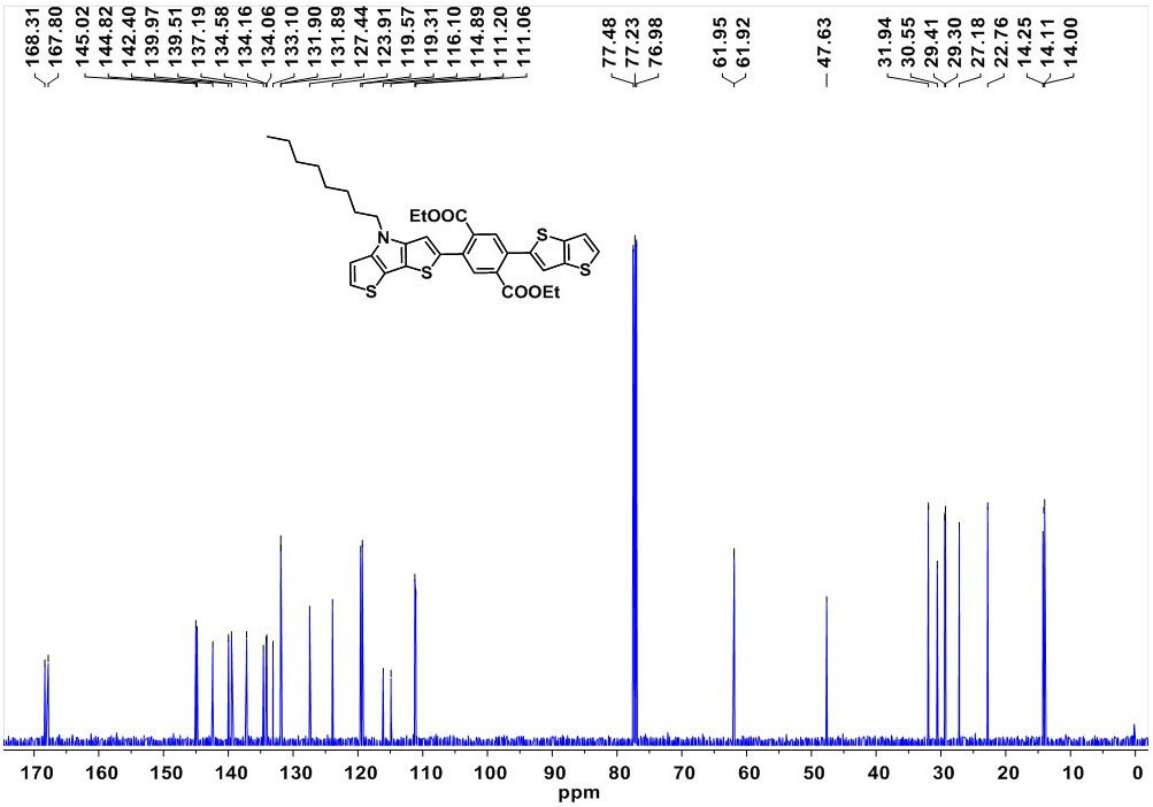

Fig. S6 ^{13}C NMR spectrum of compund 4

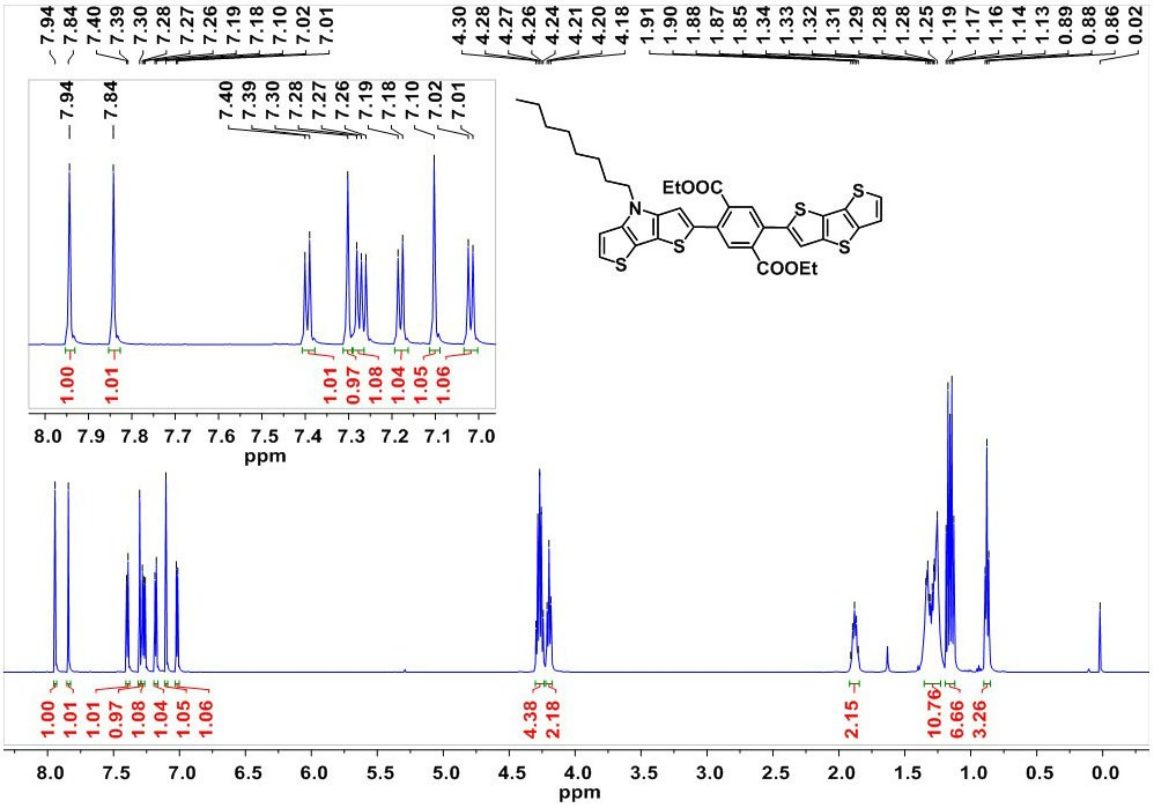

Fig. S7 ^{1}H NMR spectrum of compund 5.

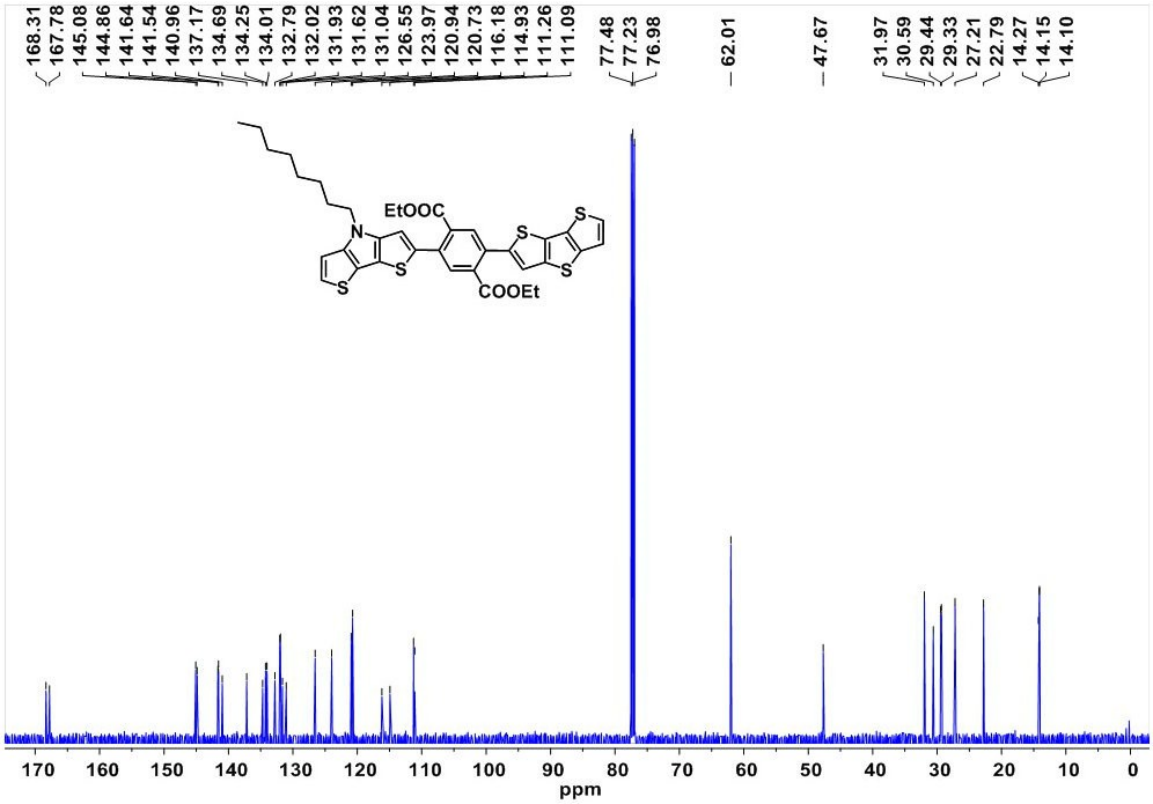

Fig. S8 ^{13}C NMR spectrum of compund 5.

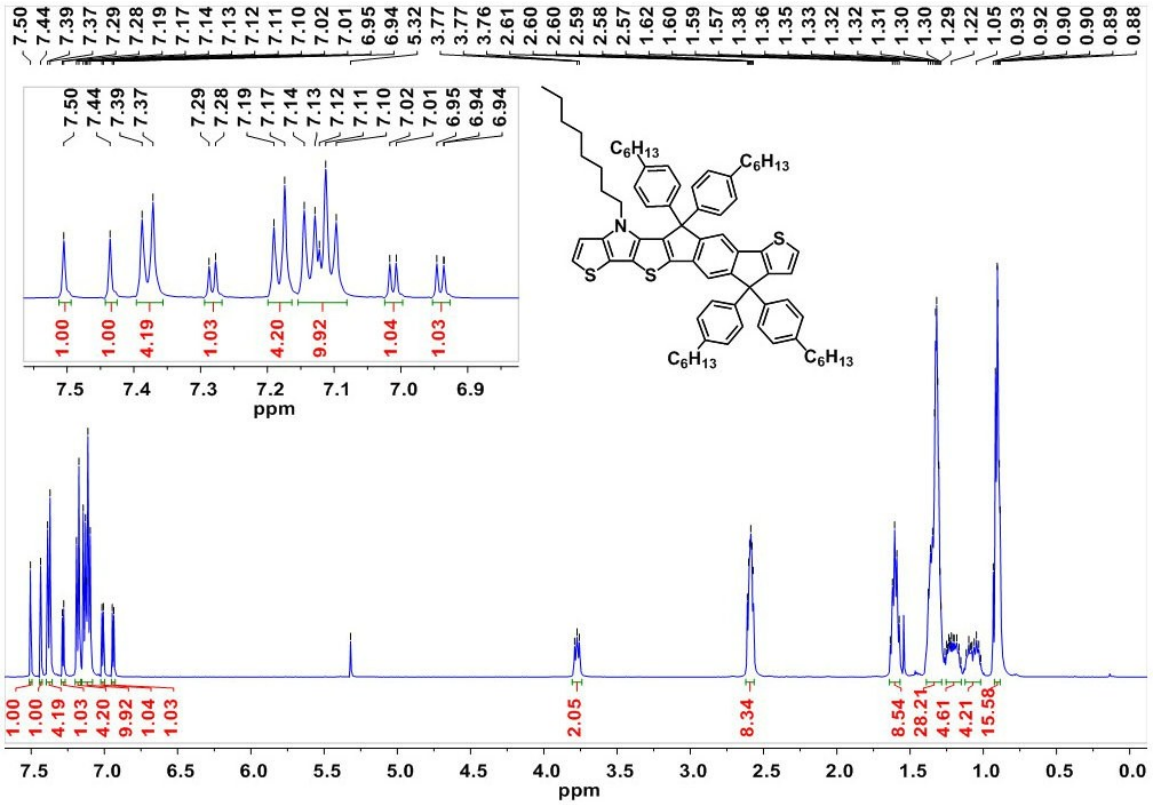

Fig. S9 ^{1}H NMR spectrum of IPT.

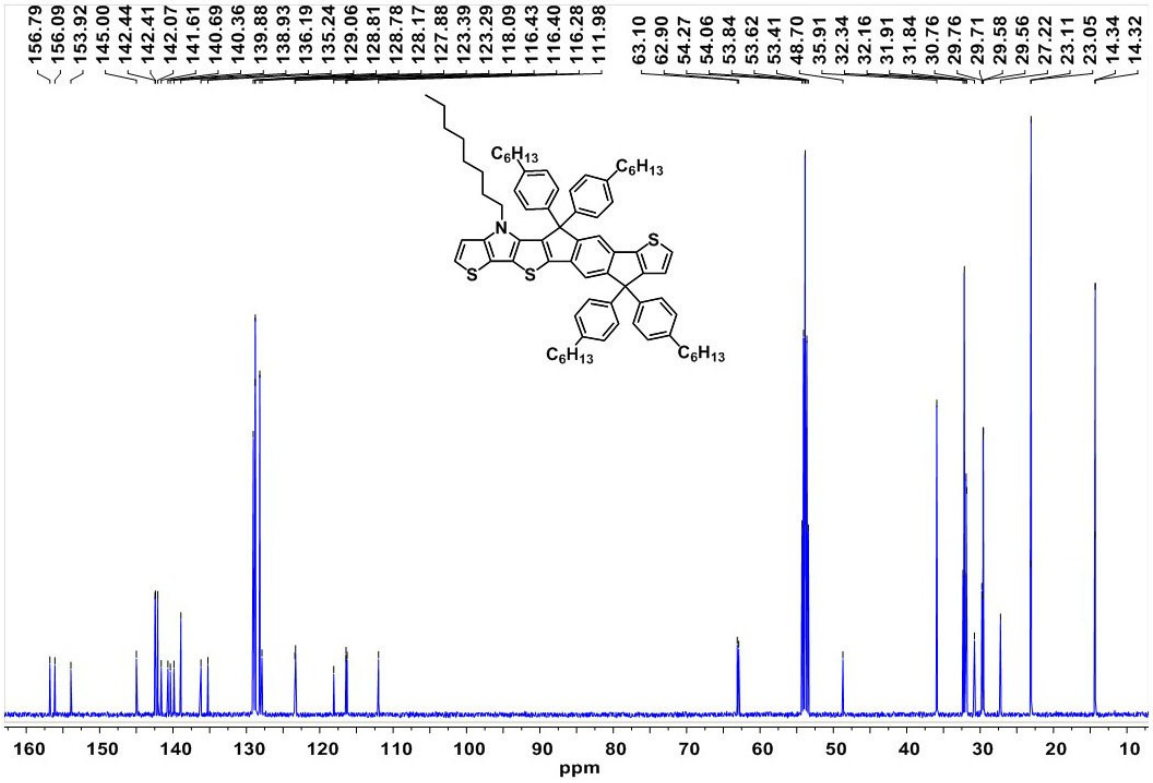

Fig. S10 ^{13}C NMR spectrum of IPT.

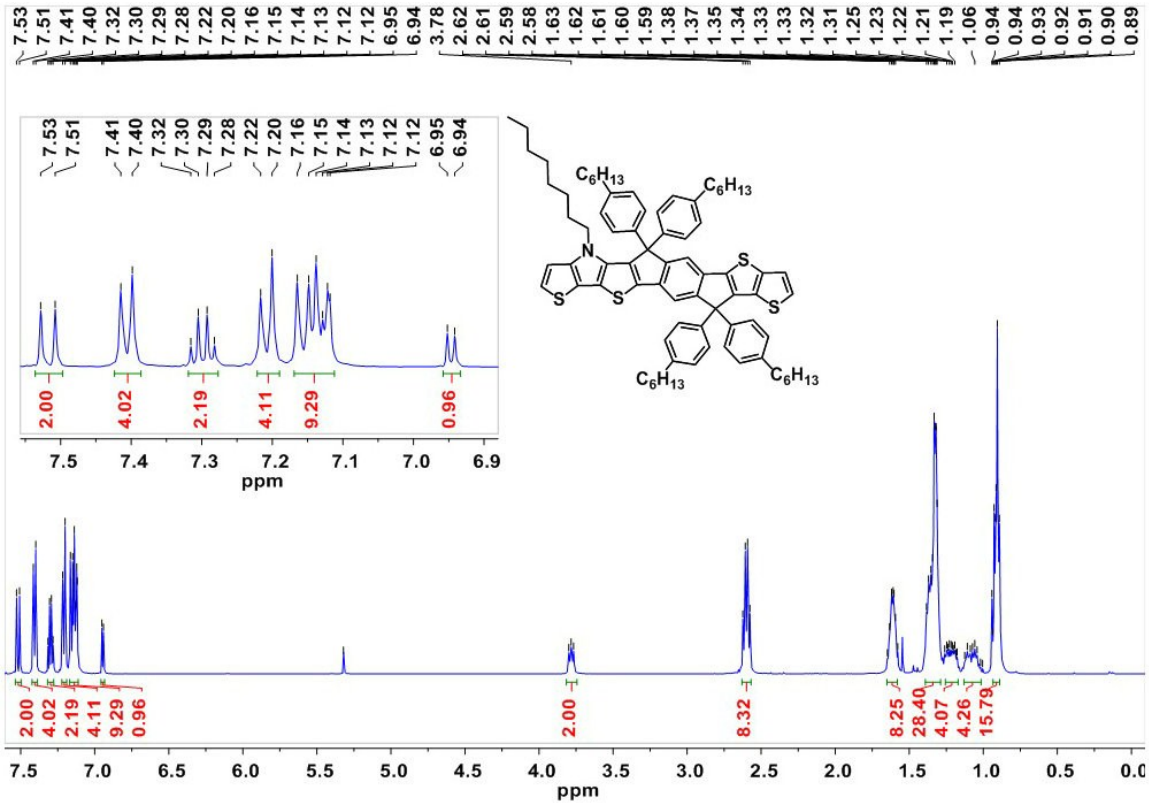

Fig. S11 ^{1}H NMR spectrum of IPTT.

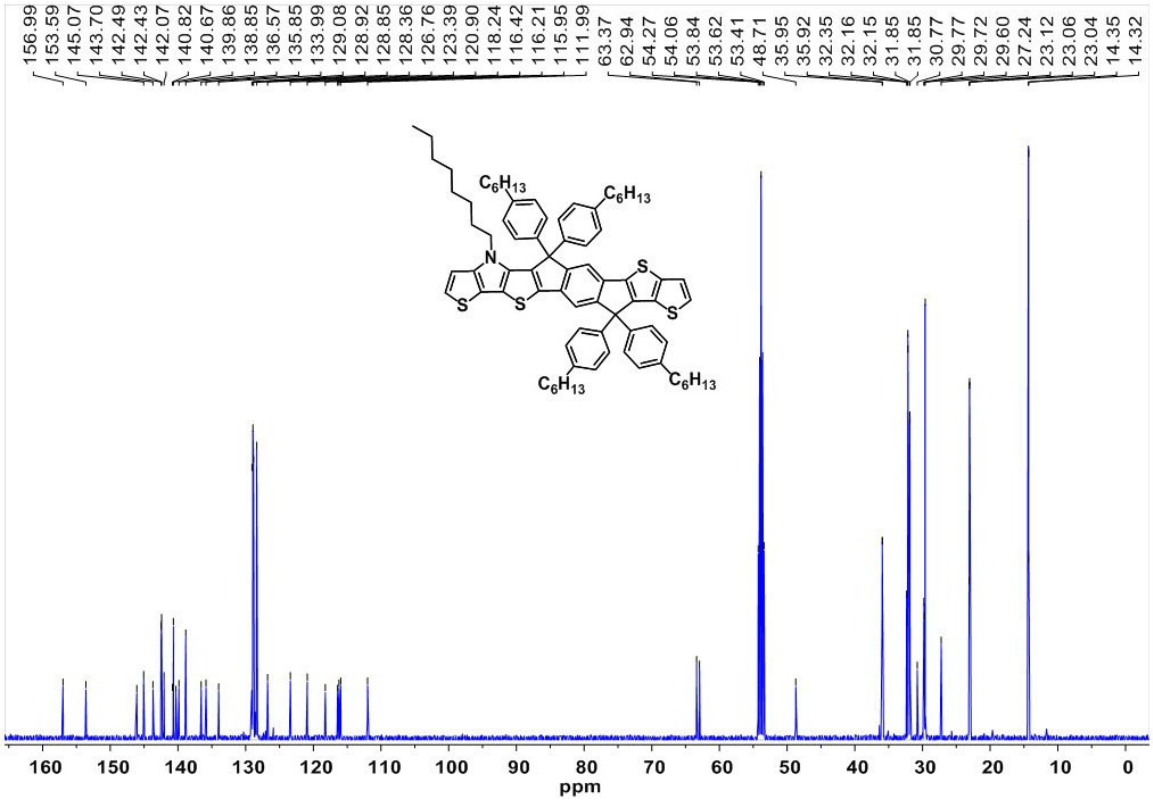

Fig. S12 ^{13}C NMR spectrum of IPTT.

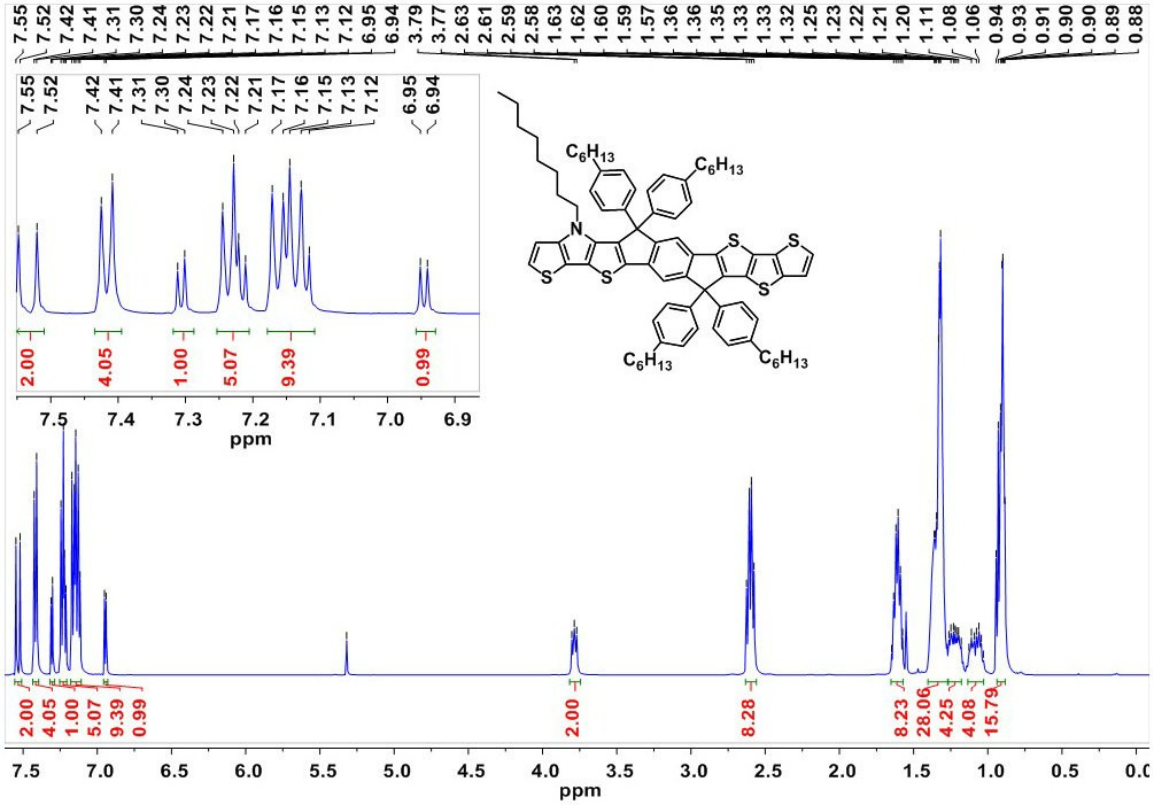

Fig. S13 ^{1}H NMR spectrum of IPTTT.

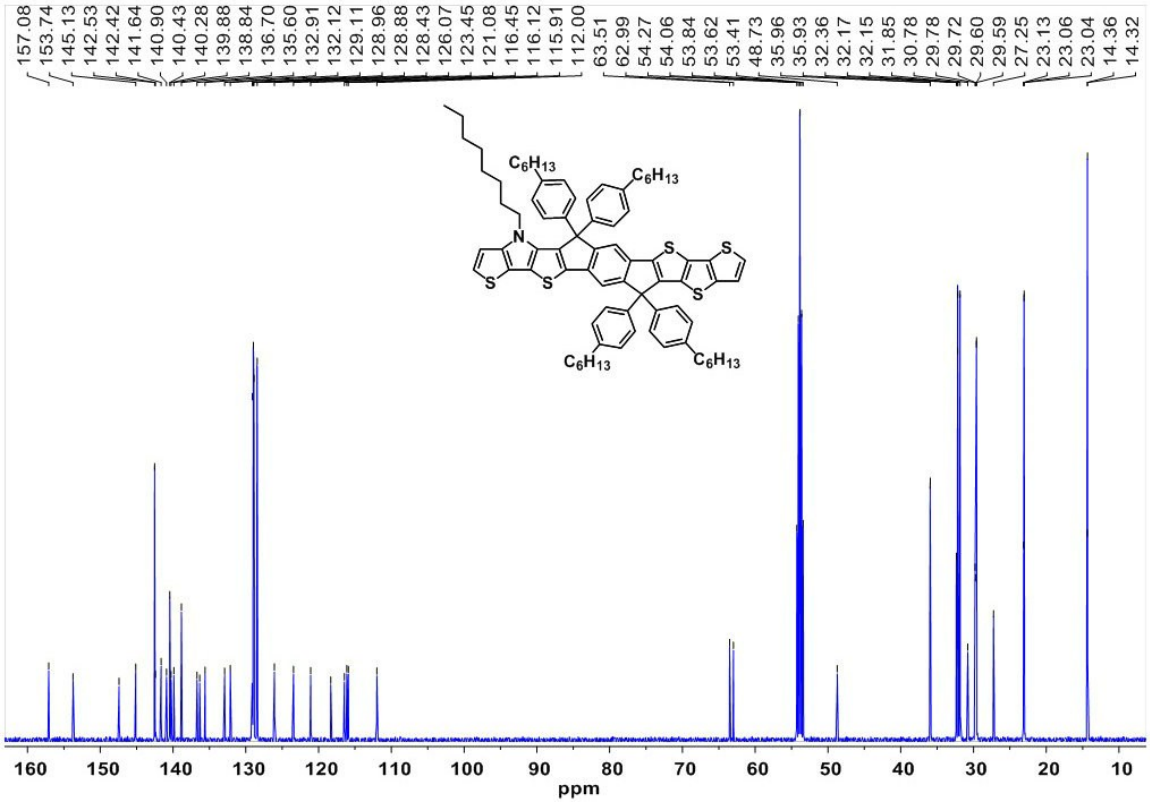

Fig. S14 ^{13}C NMR spectrum of IPTTT.

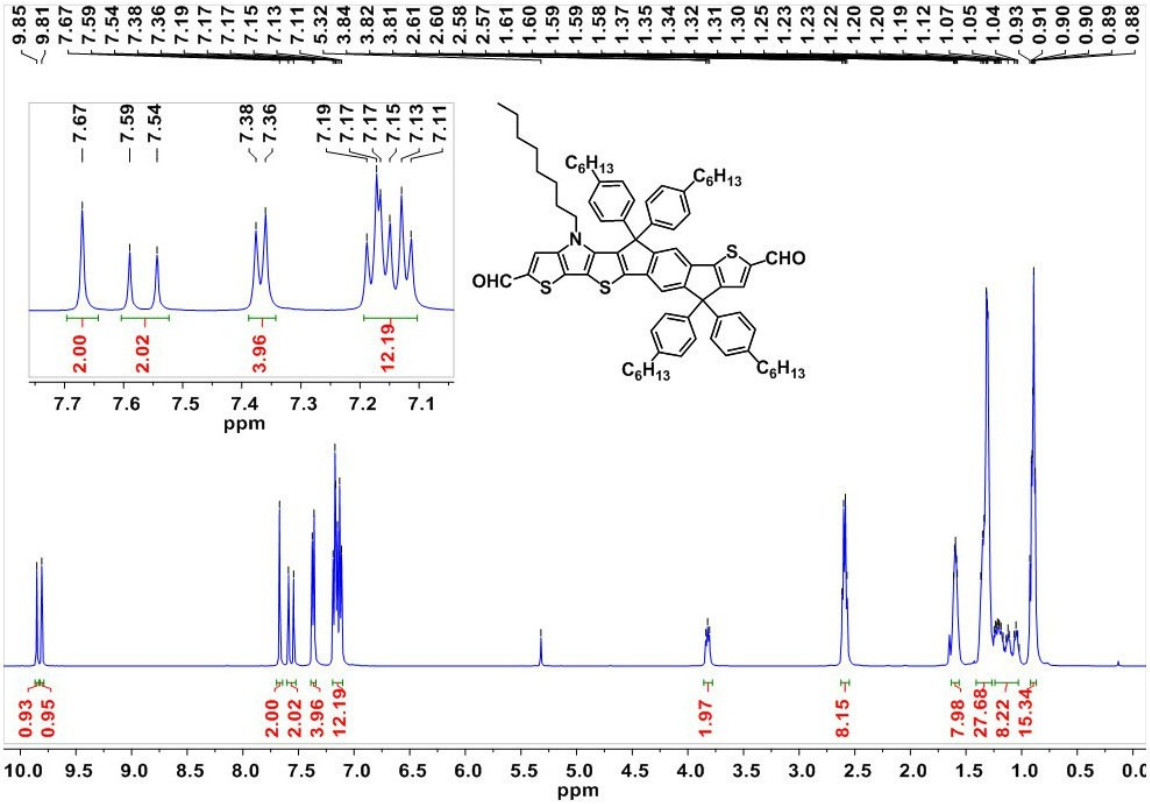

Fig. S15 ^{1}H NMR spectrum of IPT-CHO.

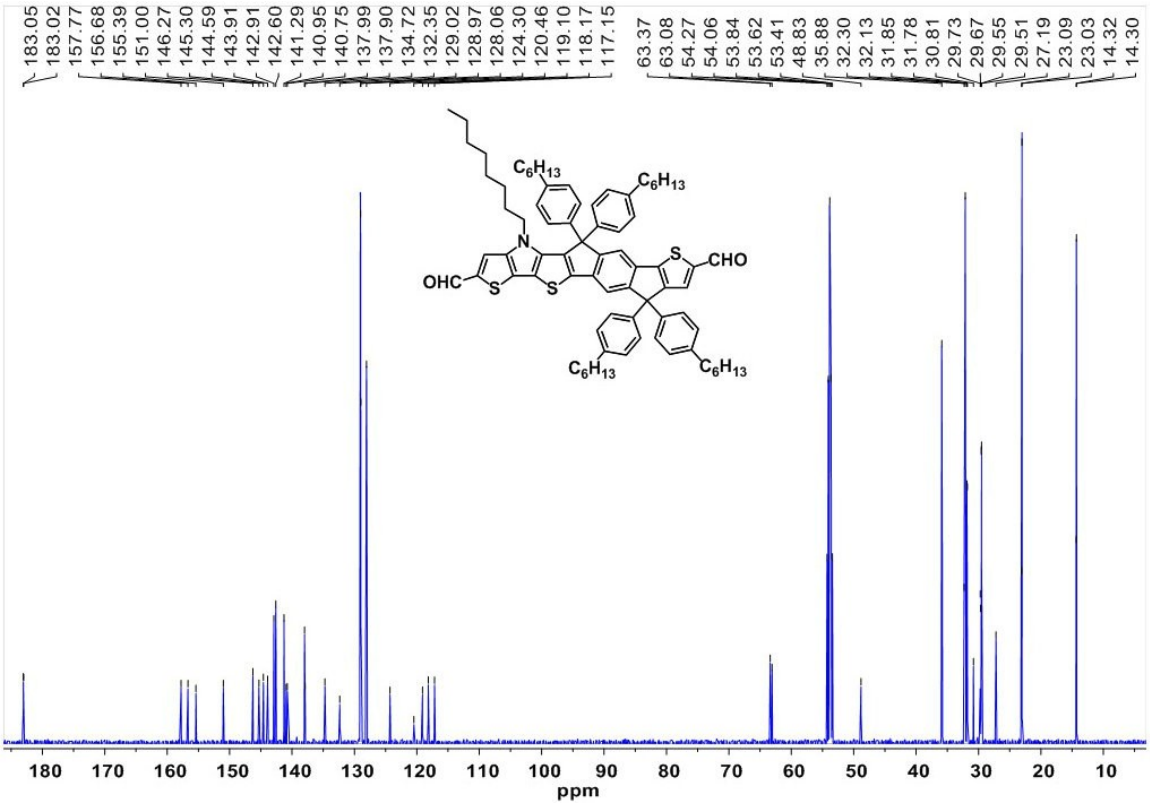

Fig. S16 ^{13}C NMR spectrum of IPT-CHO.

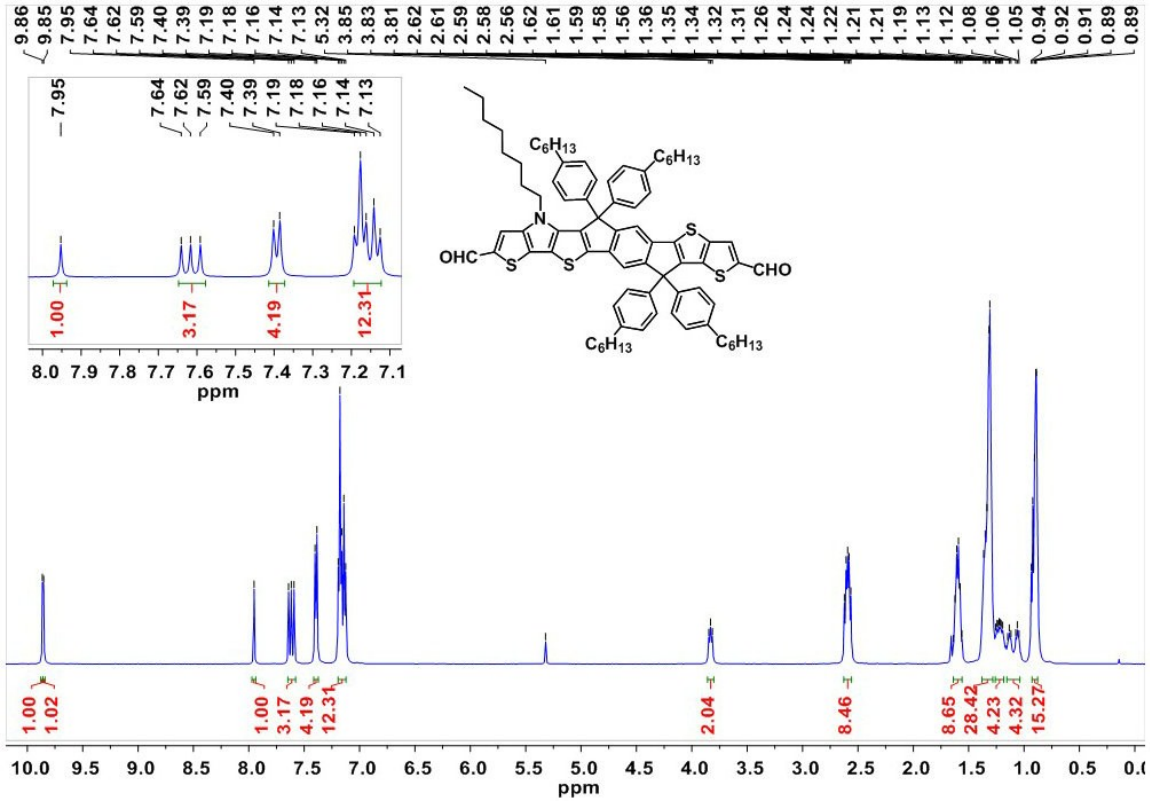

Fig. S17 ^{1}H NMR spectrum of IPTT-CHO.

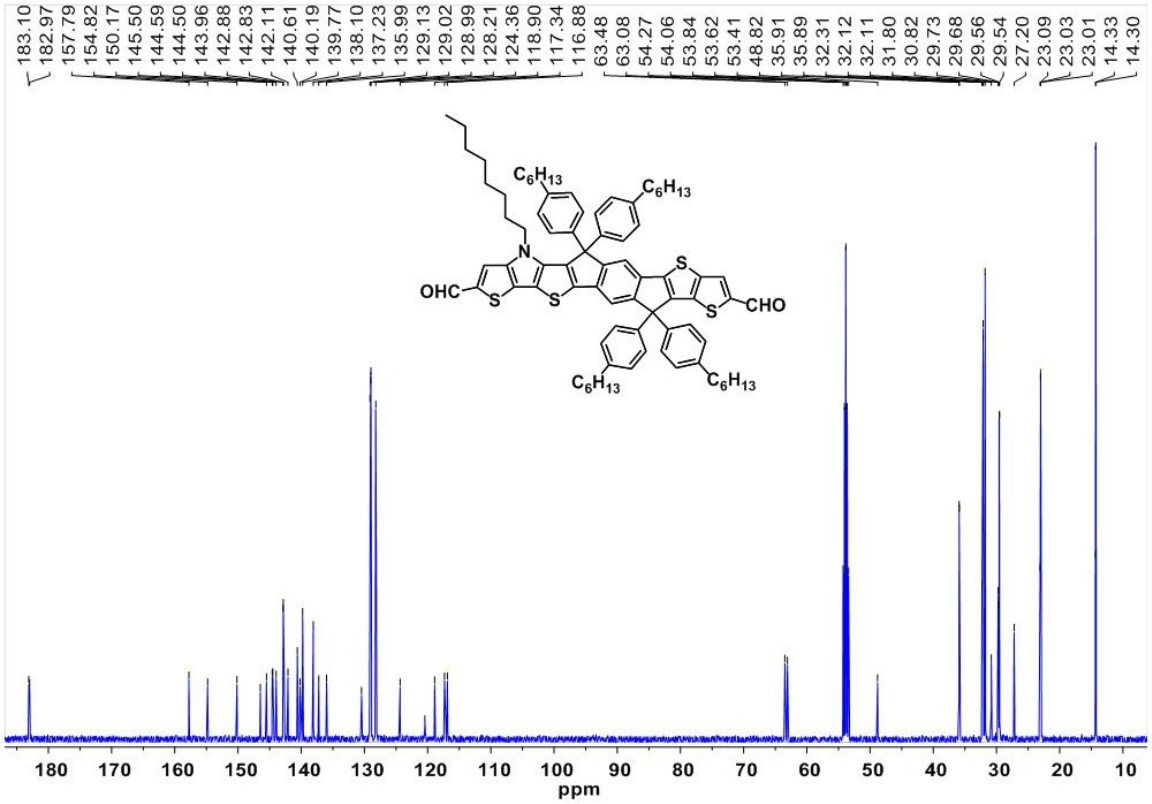

Fig. S18 ^{13}C NMR spectrum of IPTT-CHO.

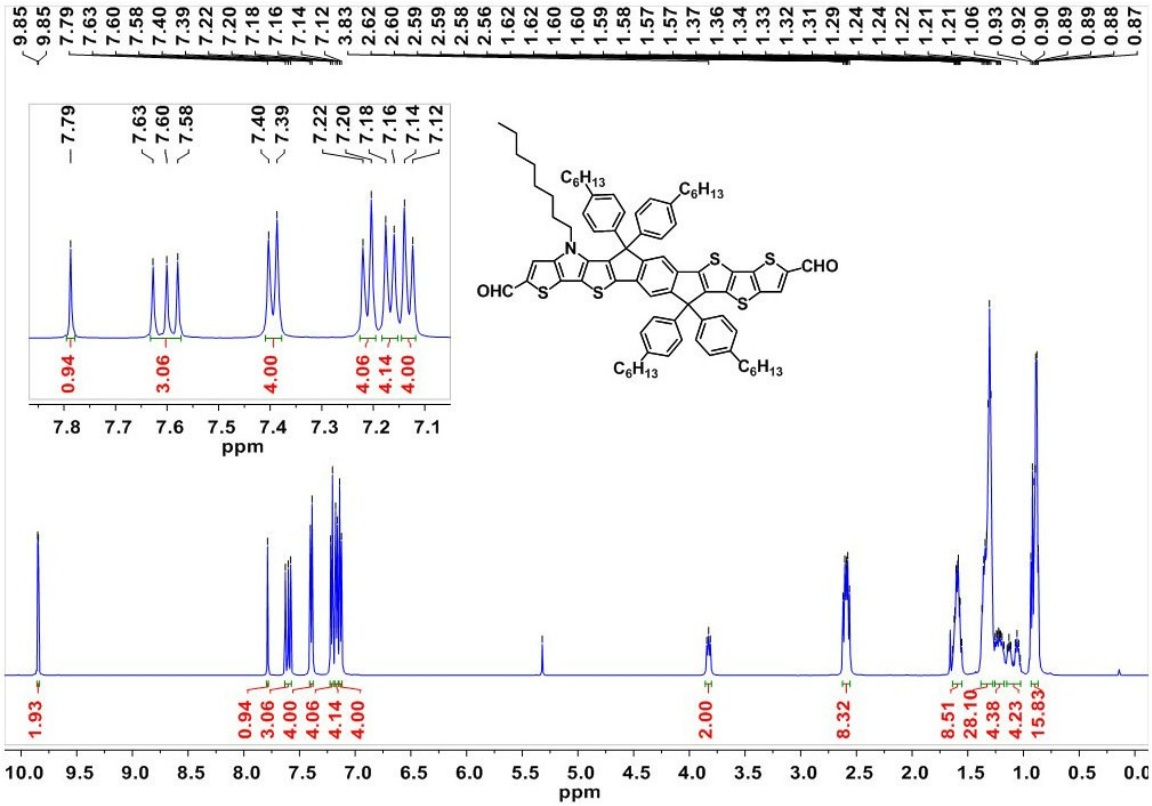

Fig. S19 ^{1}H NMR spectrum of IPTTT-CHO.

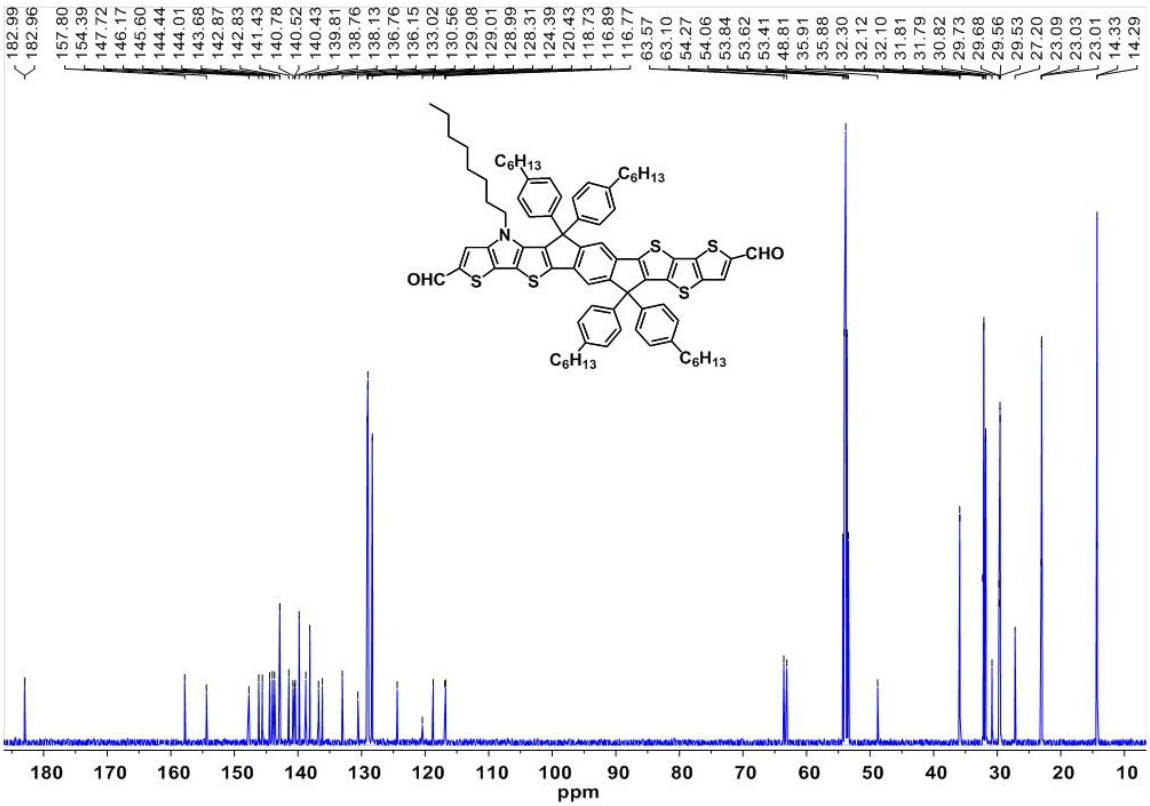

Fig. S20 ^{13}C NMR spectrum of IPTTT-CHO.

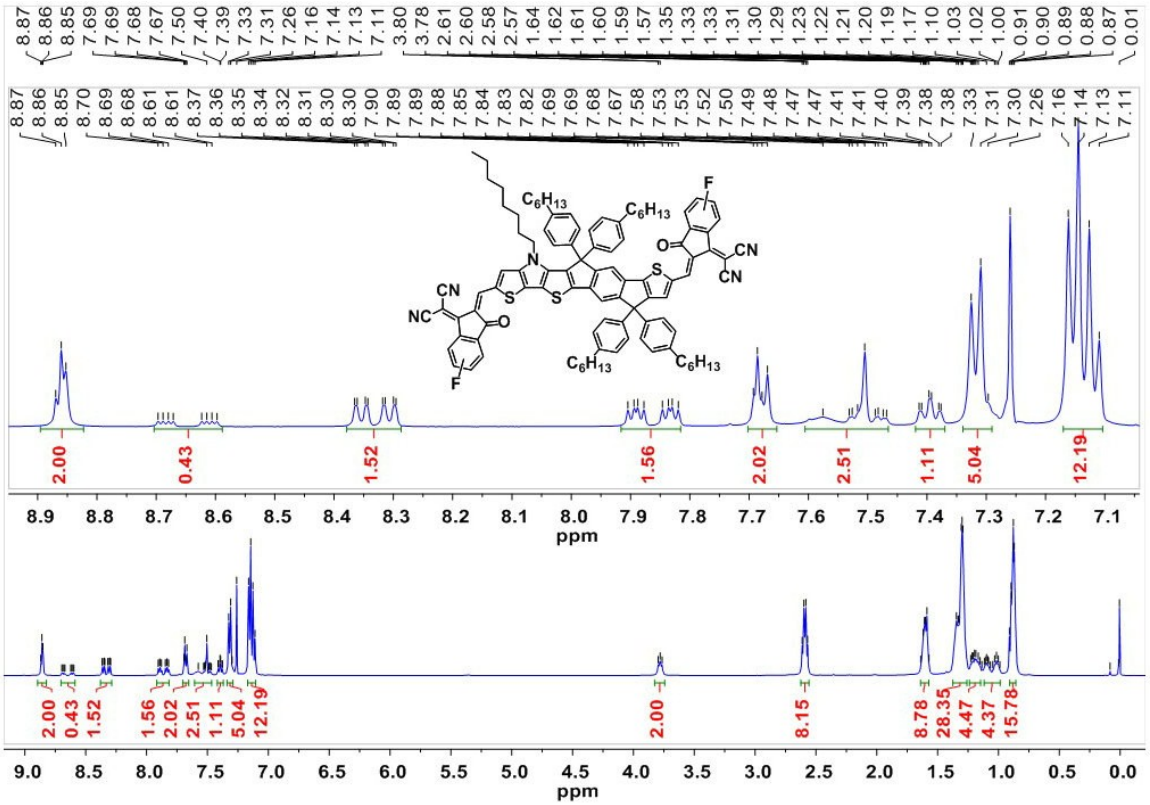

Fig. S21 ^{1}H NMR spectrum of IPT-2F.

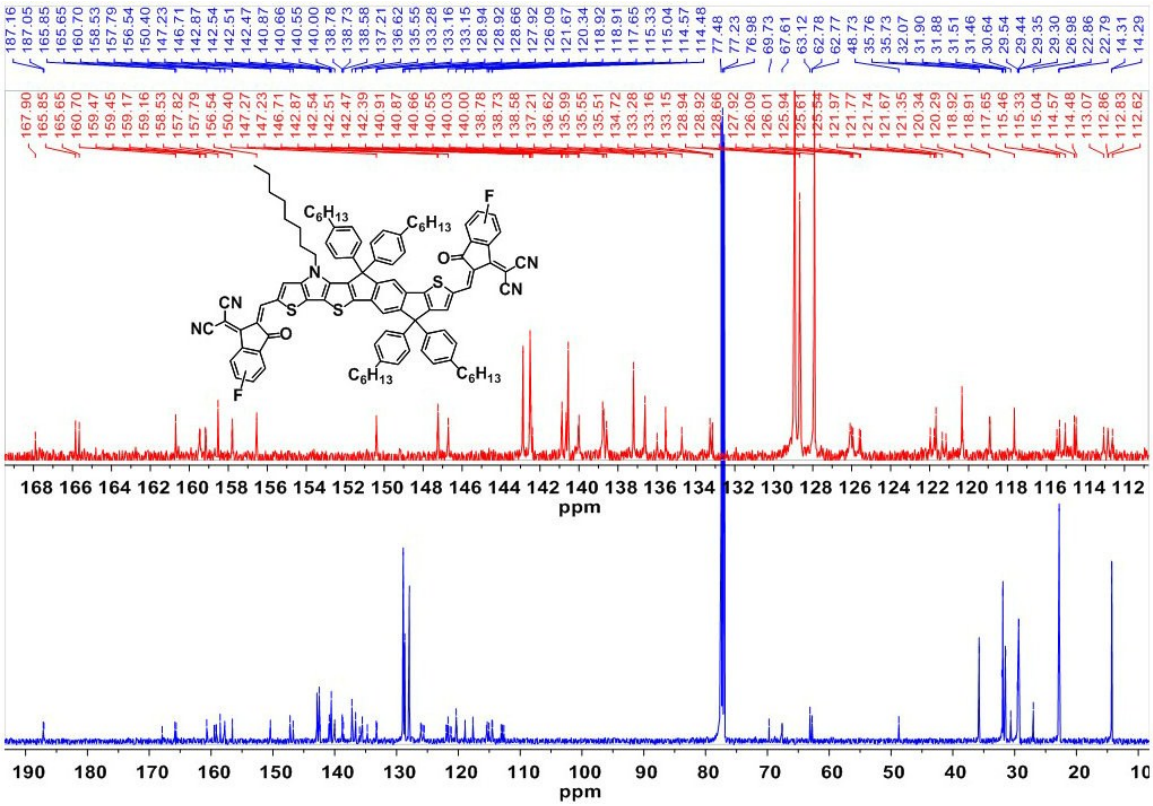

Fig. S22 ^{13}C NMR spectrum of IPT-2F.

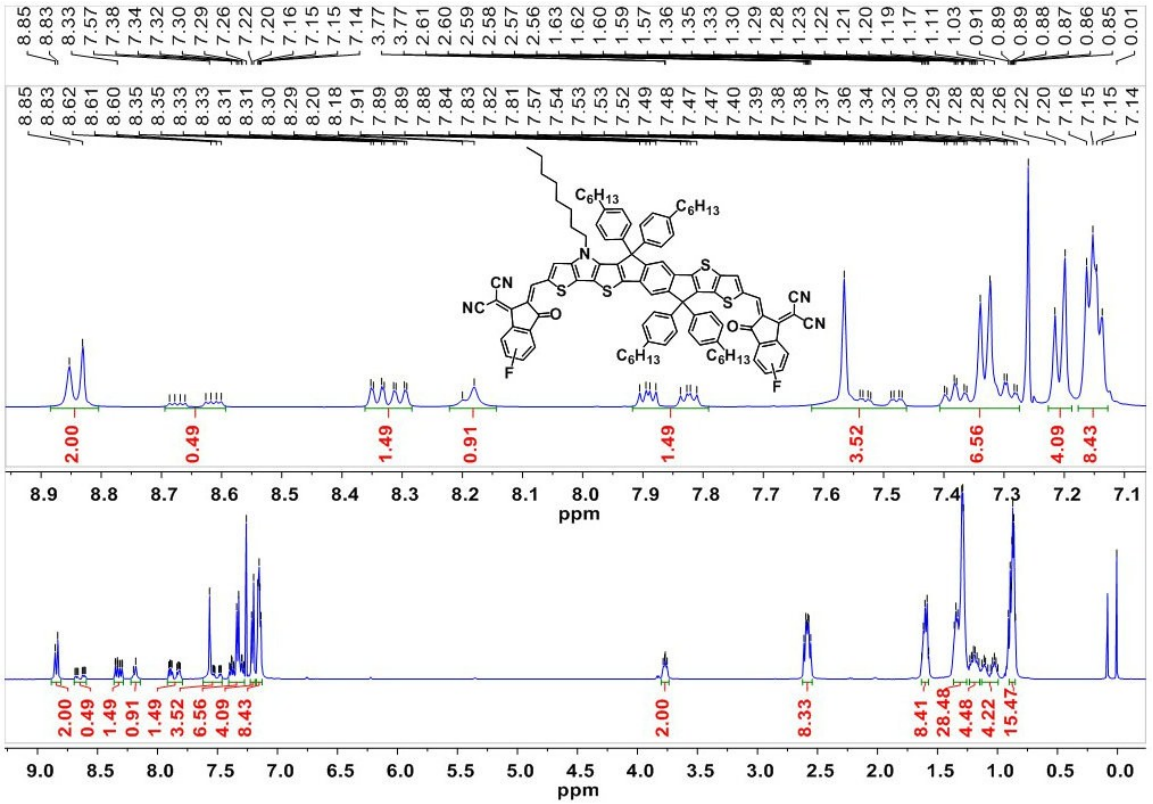

Fig. S23 ^{1}H NMR spectrum of IPTT-2F.

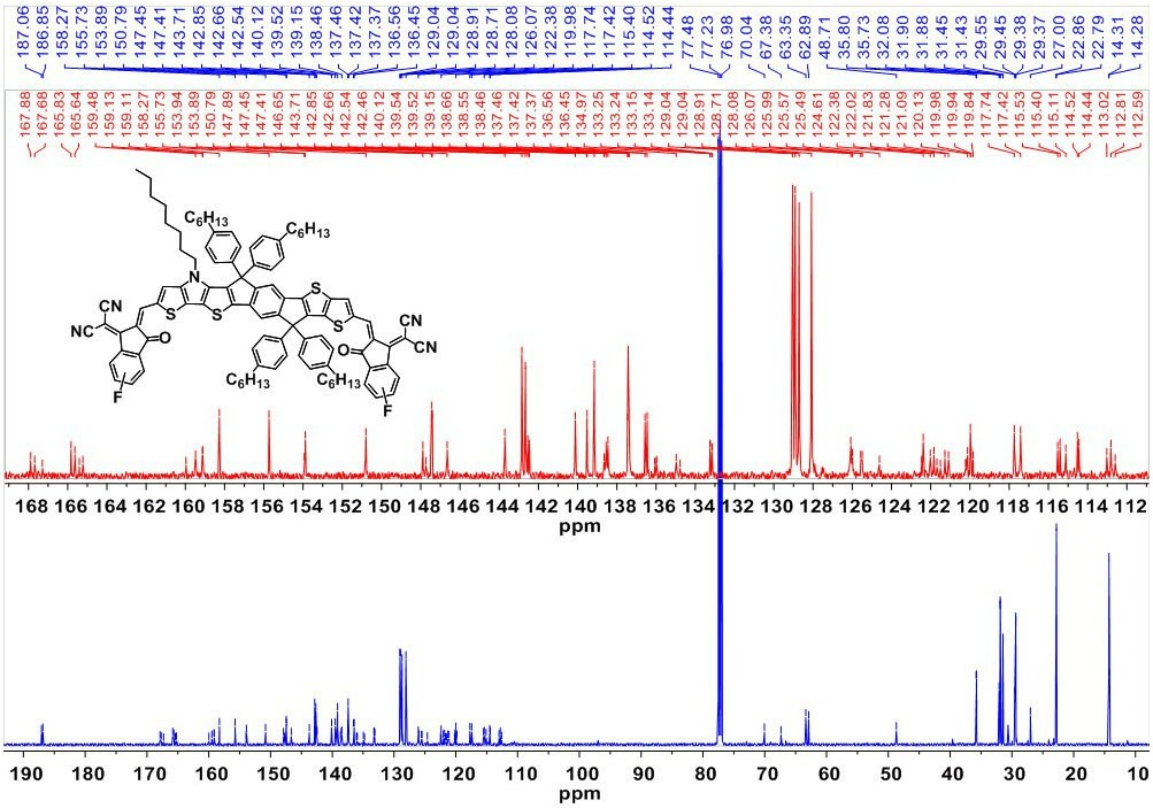

Fig. S24 ^{13}C NMR spectrum of IPTT-2F.

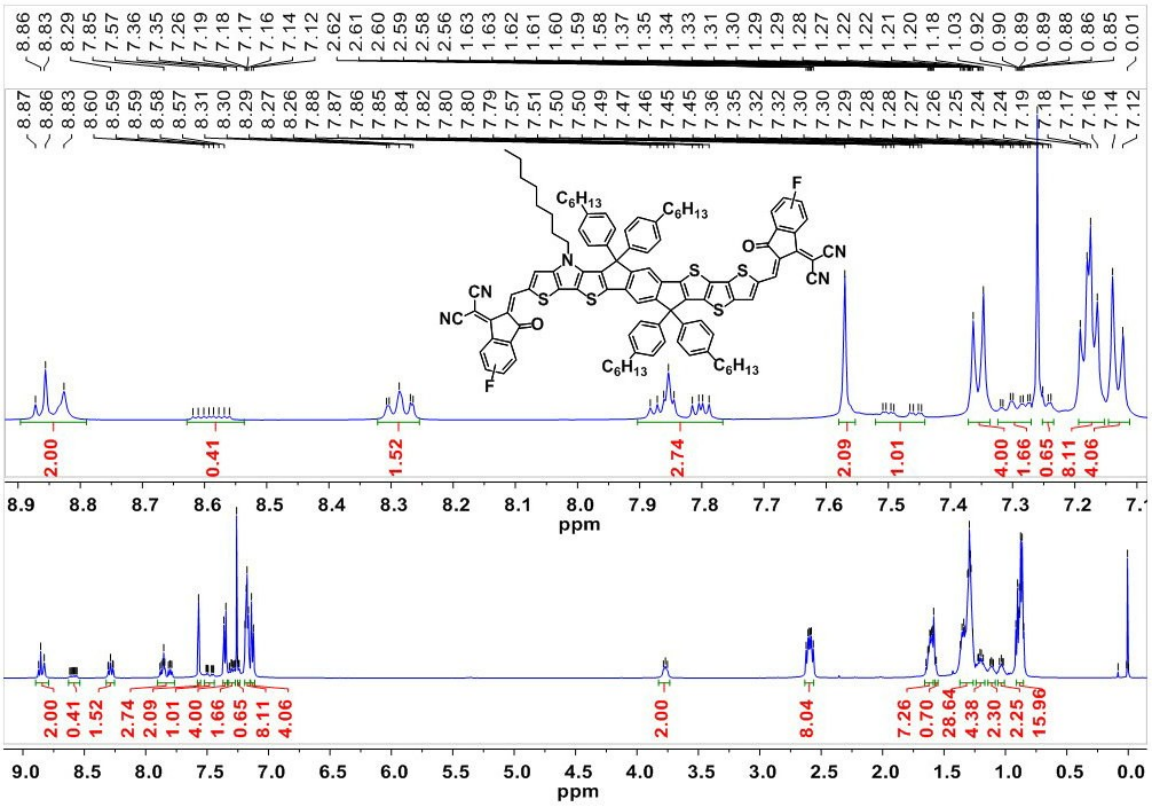

Fig. S25 ^{1}H NMR spectrum of IPTTT-2F.

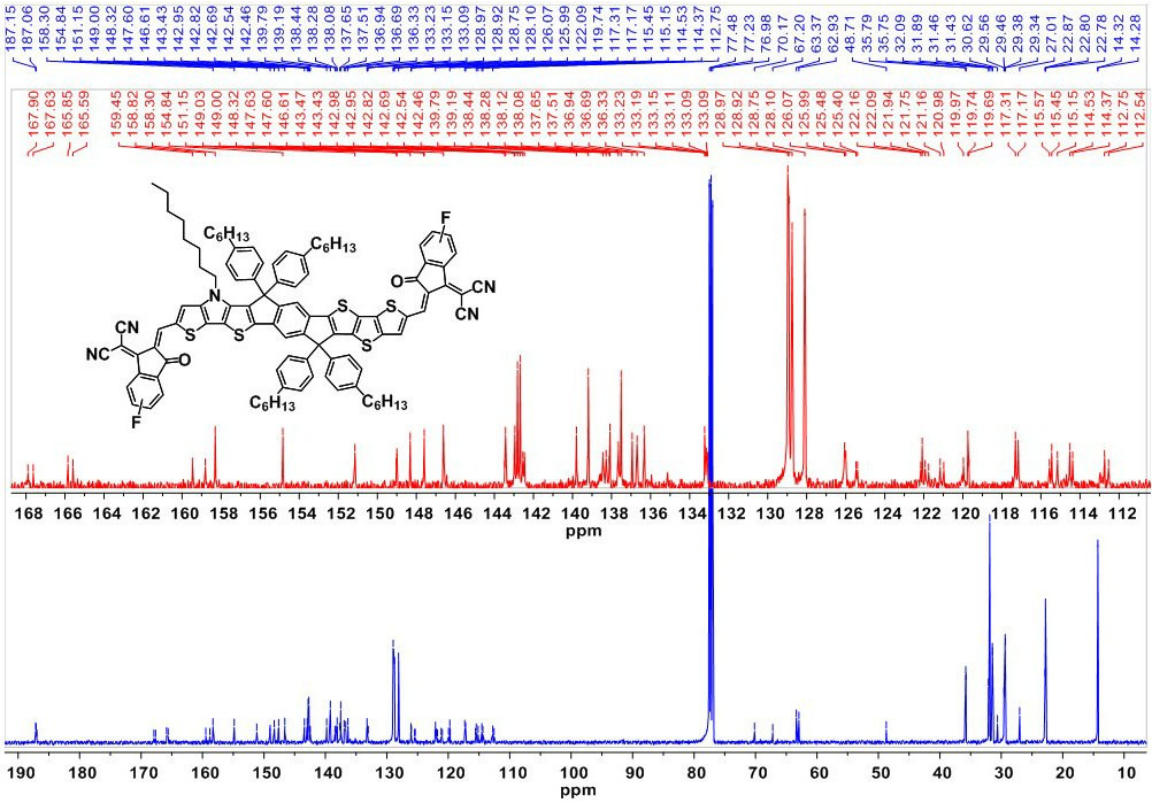

Fig. S26 ^{13}C NMR spectrum of IPTTT-2F.

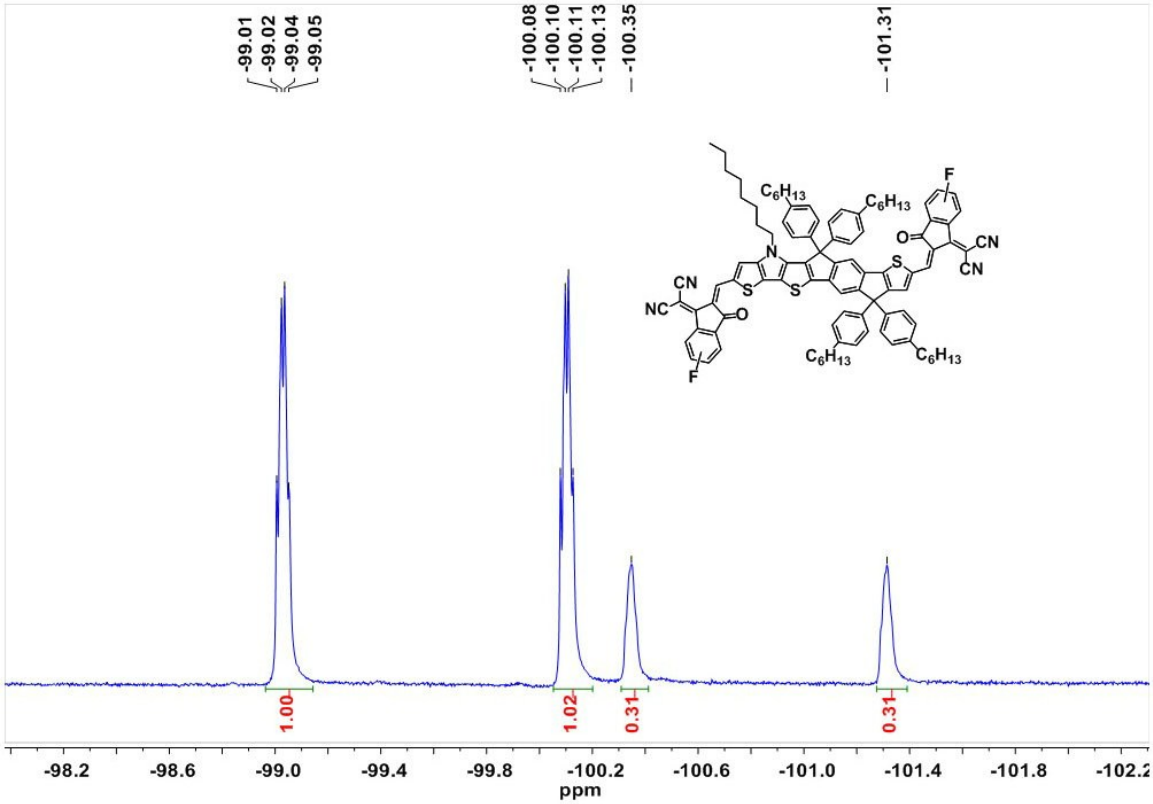

Fig. S27 ^{19}F NMR spectrum of IPT-2F.

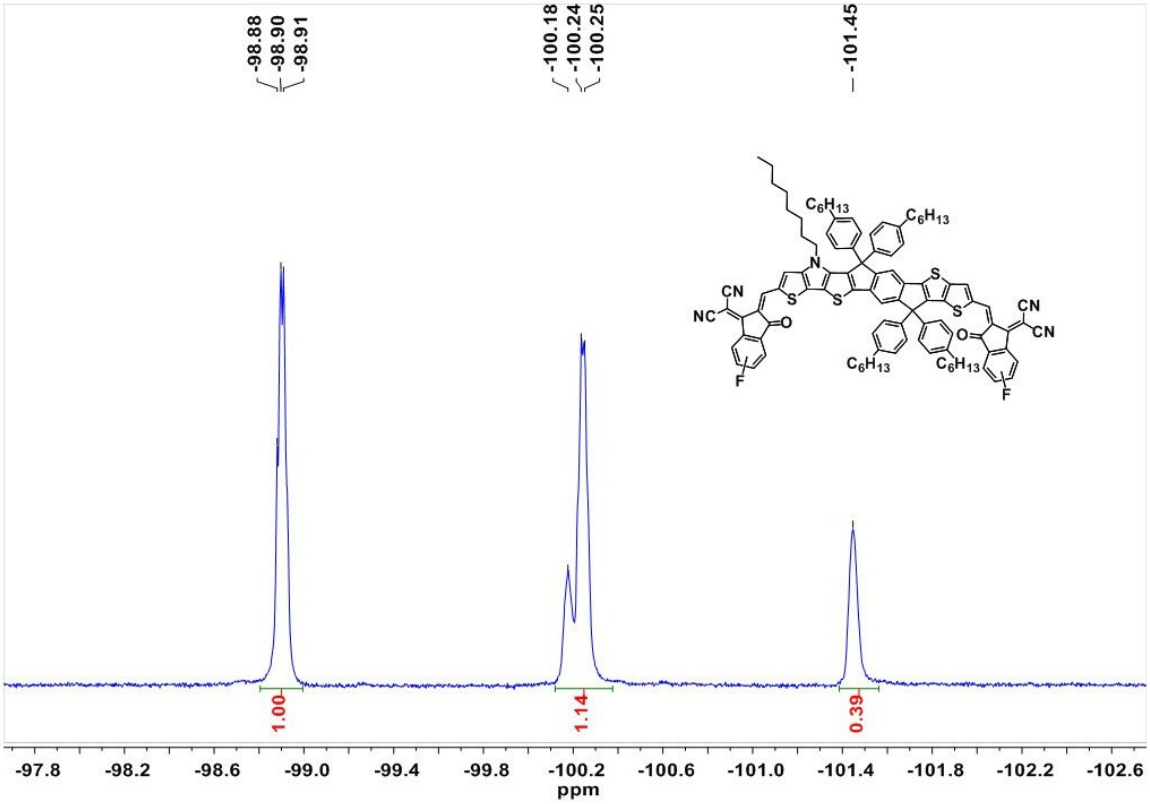

Fig. S28 ^{19}F NMR spectrum of IPTT-2F.

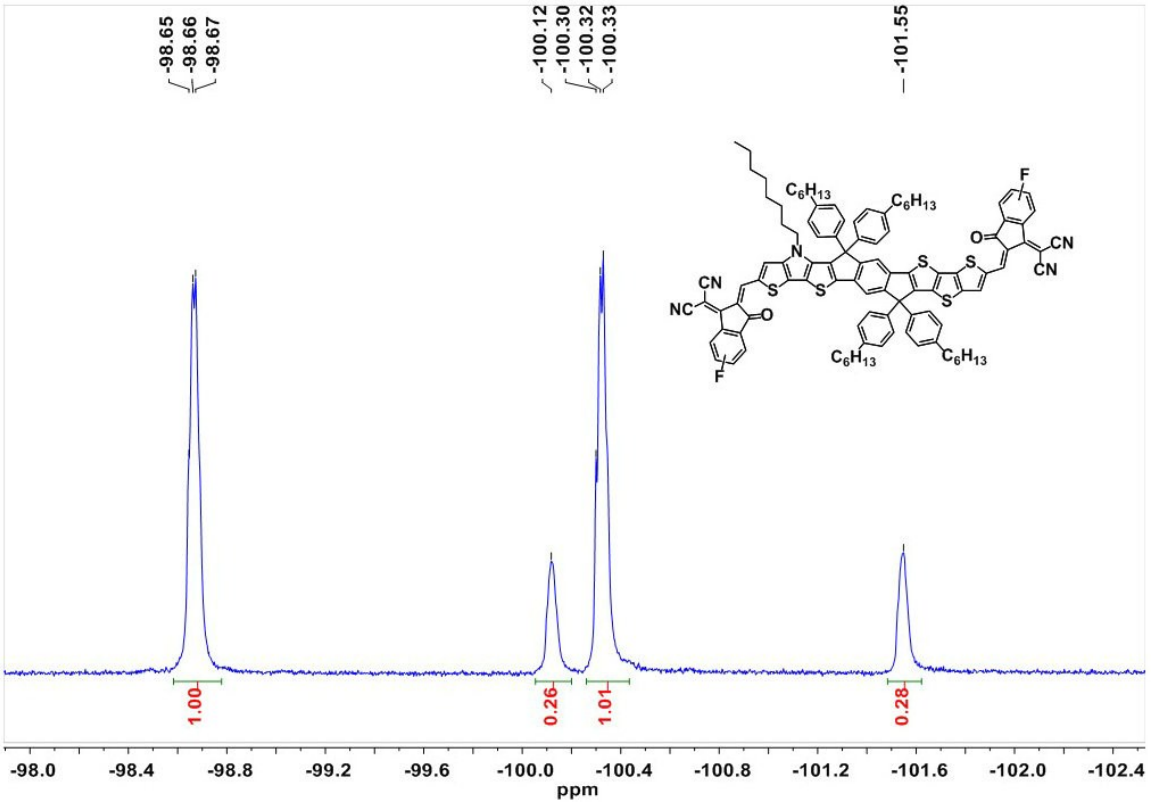

Fig. S29 ^{19}F NMR spectrum of IPTTT-2F.

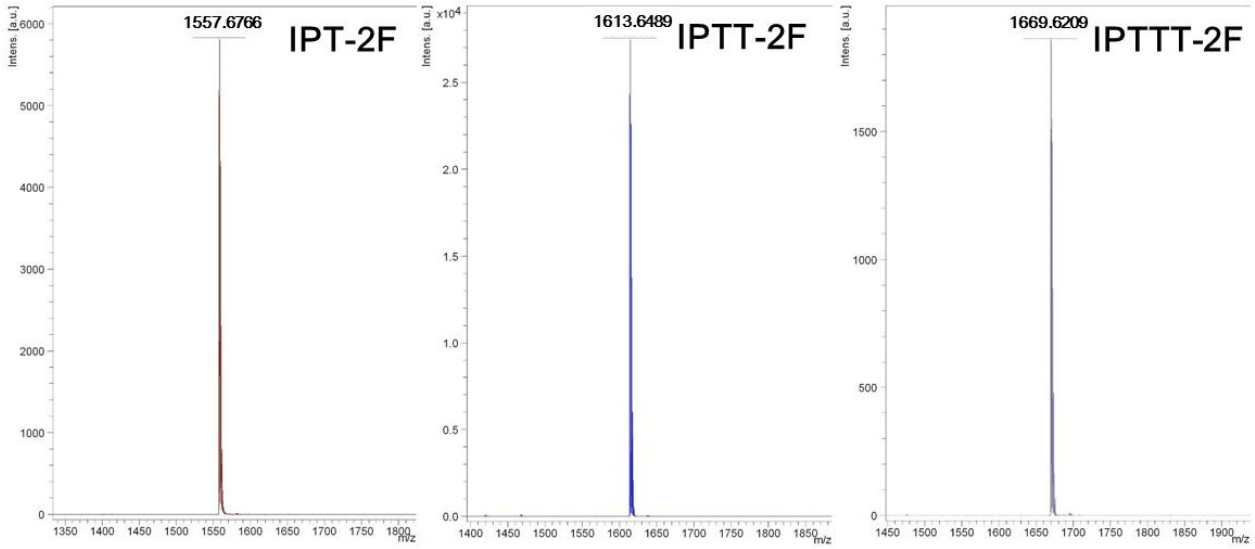

Fig. S30 MALDI-TOF MS plots

4. TG Analysis, CV Measurement and DSC Measurement

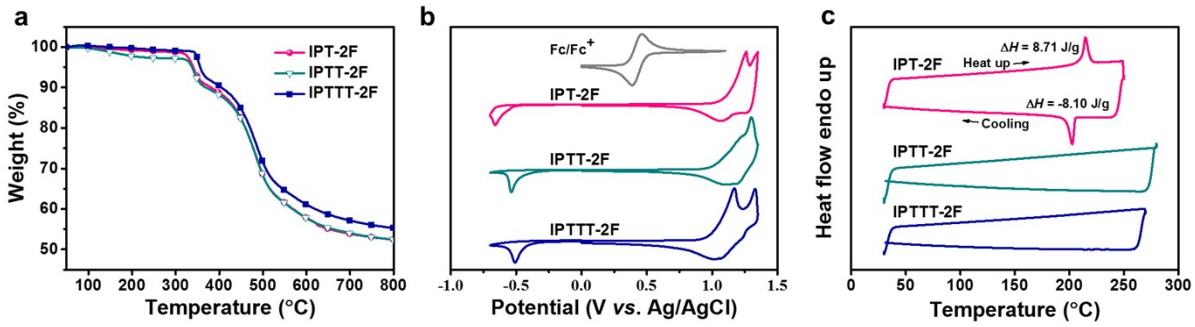

Fig. S31 a) Thermogravimetric analysis plots. b) Cyclic voltammetry plots. c) Differential scanning calorimeter plots.

5. Absorption and Photovoltaic Parameters Comparison

Table S1 Performance comparision in similar structure FREAs replaced thiophene ring with pyrrole ring.

Acceptors	λ_{max} [b] [nm]	E_g^{opt} [c] [eV]	J_{SC} [mA cm^{-2}]	PCE [%]	Reference
IPT-2F	**775**	**1.44**	**22.4**	**14.0**	**This work**
TPTTT-2F[c]	724	1.56	17.6	12.0	[4]
IPTT-2F	**766**	**1.42**	**19.0**	**11.4**	**This work**
TTPTTT-2F[c]	726	1.54	16.8	11.5	[5]
IPTTT-2F	**761**	**1.43**	**19.2**	**12.3**	**This work**
INIC2 (TTTPTTT-2F) [d]	728	1.52	17.6	10.8	[6]
ITIC3 (TTPTT-2F) [e]	734	1.55	16.8	8.1	[7]
IT-2F (TTPTT-2F) [f]	—	—	19.6	12.7	[8]

[a] In thin film. [b] E_g^{opt} =1240/λ_{onset}. [c] OSCs based on polymer donor PBT1-C. [d] OSCs based on polymer donor FTAZ. [e] as-cast OSCs based on polymer donor PTB7-Th. [f] OSCs based on polymer donor PBDB-TF.

6. Device Fabrication and Measurement

The device structure is indium tin oxide (ITO)/PEDOT:PSS/PBDB-T:acceptors/Phen-NaDPO/Ag. Phen-NaDPO were purchased

from 1-Materials Inc. The PBDB-T and the three SMAs (IPT-2F, IPTT-2F, and IPTTT-2F) were blended at a donor/acceptor (D/A) ratio of 1:1 and dissolved in chlorobenzene to obtain a solution with a total concentration of 20 mg/mL. 1,8 diiodooctane (DIO) was added as a solvent additive at 0.5% volume of the blend solution. The patterned ITO-coated glass substrates (15 Ω per square) were cleaned with detergent water, deionized water, acetone and isopropyl alcohol in an ultrasonic bath sequentially for 20 minutes, and then under UV-Ozone treatment for 15 minutes. After the UV-Ozone treatment, PEDOT:PSS solution was spin-coated at 4000 rpm onto the ITO substrates. After being baked at 150°C for 10 min in air, the PEDOT:PSS-coated substrates were transferred into nitrogen-filled glove box. The donor/acceptor blend solution was spin-coated with 2000 rpm. For Phen-NaDPO interface, we spin-coated the solution with 4000 rpm on top of the active layer, then deposited 100 nm Ag by thermal evaporation.

J-V measurements of solar cells were performed in the glovebox with a Keithley 2400 source meter and an Oriel Sol3A Class AAA solar simulator calibrated to 1 sun, AM1.5 G. The external quantum efficiency (EQE) measurements were performed at zero bias by illuminating the device with monochromatic light supplied from a Xenon arc lamp in combination with a dual-grating monochromator. The number of photons incident on the sample was calculated for each wavelength by using a silicon photodiode calibrated by NIST. Electron-only devices with the structure of ITO/ZnO/Active layer/Ca/Al and hole-only devices with the structure of ITO/PEDOT:PSS/Active layer/MoOx/Ag were used to evaluate charge mobility by SCLC model. A 5400 Agilent atomic force microscopy (AFM) instrument was performed to obtain morphology images.

Table S2 Device data of OSCs based on PBDB-T/IPT-2F with different DIO content.

DIO [v/v]	J_{SC} [mA cm^{-2}]	V_{OC} [V]	FF [%]	PCE [%]
0	19.5	862	67.2	11.3
0.5	21.4	860	68.3	12.6
1	20.4	854	62.4	10.9

Table S3 Device data of OSCs based on PBDB-T/IPT-2F with different annealing temperature.

Annealing [°C]	J_{SC} [mA cm^{-2}]	V_{OC} [V]	FF [%]	PCE [%]
80	21.8	862	70.4	13.2
100	22.0	856	71.9	13.5
120	20.5	854	68.4	12.0

Table S4 Device data of OSCs based on PBDB-T/Acceptor with different D/A weight ratio.

Acceptor	D/A [w/w]	J_{SC} [mA cm^{-2}]	V_{OC} [V]	FF [%]	PCE [%]
IPT-2F	1:0.8	21.9	860	70.6	13.3
	1:1	22.4	860	72.4	14.0
	1:1.2	22.0	856	71.9	13.5
IPTT-2F	1:0.8	19.2	870	65.1	10.9
	1:1	19.7	874	66.2	11.4
	1:1.2	18.5	872	65.2	10.5
IPTTT-2F	1:0.8	18.4	892	64.5	10.6
	1:1	20.0	894	69.3	12.3
	1:1.2	18.9	892	67.5	11.4

7. Additional Figure and Tables

Table S5 Statistic data of binary single-junction OSCs based on asymmestrical FREAs.

Active layer	J_{SC} [mA cm^{-2}]	V_{OC} [V]	FF [%]	PCE [%]	Reference
PBDB-T/IPT-2F	22.4	0.860	72.4	14.0	**This work**
PBDB-TF/IT-3F [a]	20.3	0.900	75.5	13.8	[8]

PBDB-T/a-BTTIC	20.3	0.904	74.0	13.6	[9]
J71/ZITI-3F [a]	20.7	0.900	71.5	13.2	[10]
PBDB-T/MeIC1	18.3	0.927	74.1	12.6	[11]
PBDB-T/IDT8CN-M	17.1	0.920	78.9	12.4	[12]
PM6/IDT6CN-TM	17.4	0.953	74.7	12.4	[13]
PBDB-T/IPTTT-2F	20.0	0.894	69.3	12.3	**This work**
PBT1-C/SePTTT-2F	18.0	0.895	75.9	12.2	[14]
PBT1-C/TTPTTT-4F	19.4	0.863	72.1	12.1	[5]
PBDB-T/*a*-IT-2OM [a]	18.1	0.930	71.5	12.1	[15]
PBT1-C/TPTTT-2F	17.6	0.916	74.5	12.0	[4]
PBT1-C-2Cl/IDTT-2F-Th [a]	17.8	0.912	73.9	12.0	[16]
PBT1-C/TTPTTT-2F	16.8	0.920	74.6	11.5	[11]
PBDB-T/IPTT-2F	19.9	0.874	66.2	11.4	**This work**
PBDB-T/IDT6CN-M	16.0	0.910	76.8	11.2	[17]
PBDB-T/IDTT-OB [b]	16.6	0.910	74.0	11.2	[18]
PBT1-C/SePTT-2F	17.5	0.830	75.0	10.9	[11]
PM6/IDT6CN-4F	18.3	0.859	69.1	10.9	[13]
PBT1-C/TPTT-IC	15.6	0.960	70.0	10.5	[19]
PBDB-T/IDT6CN-Th	16.8	0.810	76.7	10.4	[17]
PBDB-T/*a*-IT-2F [a]	19.1	0.780	68.8	10.3	[15]
PBT1-C/TPTT-2F	15.8	0.881	73.0	10.2	[4]
PBT1-C/SePT-IN	16.4	0.850	73.3	10.2	[20]
PBDB-T/IDT-OB [b]	16.2	0.880	71.1	10.1	[21]
J71/A201	13.2	0.880	67.2	9.4	[22]
PBDB-T/IDT6CN	15.1	0.830	73.8	9.3	[17]
J71/IDTNTC	14.1	0.940	62.7	8.3	[23]
PBT1-C/TTPTTT-IC	12.1	0.996	63.7	7.9	[5]
J71/A2 [a]	11.6	0.980	39.6	4.5	[24]
J71/A1 [a]	5.7	0.970	29.6	1.6	[24]

[a] Asymmetric FREA based on two different endcapped groups. [b] FREA based on asymmetric side chains.

Table S6 OSC performance of DTP-based FREAs.

Active layer	J_{SC} [mA cm^{-2}]	V_{OC} [V]	FF [%]	PCE [%]	Reference
PBDB-T/IPT-2F	22.4	0.860	72.4	14.0	**This work**
PBDB-T/IPIC-4Cl	22.2	0.813	74.0	13.4	[25]
PBDB-T/SN6IC-4F	23.2	0.780	73.0	13.2	[26]
PBDB-T/INPIC-4F	21.6	0.850	71.5	13.1	[1]
PBDB-T/IPTTT-2F	20.0	0.894	69.3	12.3	**This work**
PBDB-T/INPIC-EH	20.7	0.837	68.4	11.9	[27]
PBDB-T/IPTT-2F	19.9	0.874	66.2	11.4	**This work**
PBDB-T/INPIC-BO	20.0	0.839	66.8	11.2	[27]
PBDB-T/IPIC-4F	19.8	0.835	67.1	11.1	[25]

PBDB-T/SN6IC	16.5	0.880	66.0	9.6	[26]
PBDB-T/INPIC	8.6	0.960	52.5	4.3	[1]
PBDB-T/IPIC	7.2	0.950	58.6	4.0	[25]

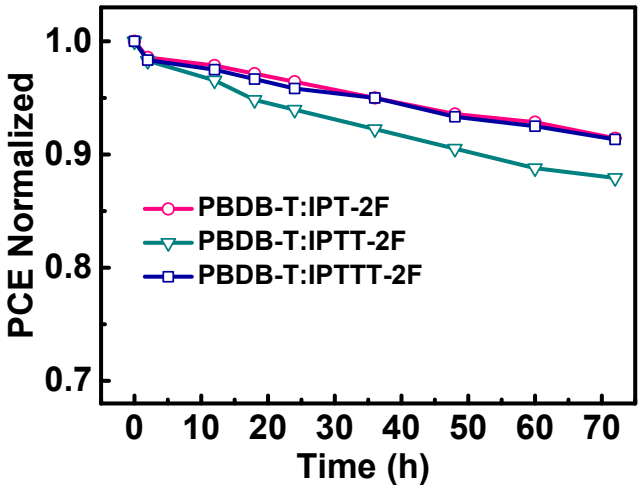

Fig. S32 Storage stability test under the condition of dark, nitrogen atmosphere and room temperature for 72 h.

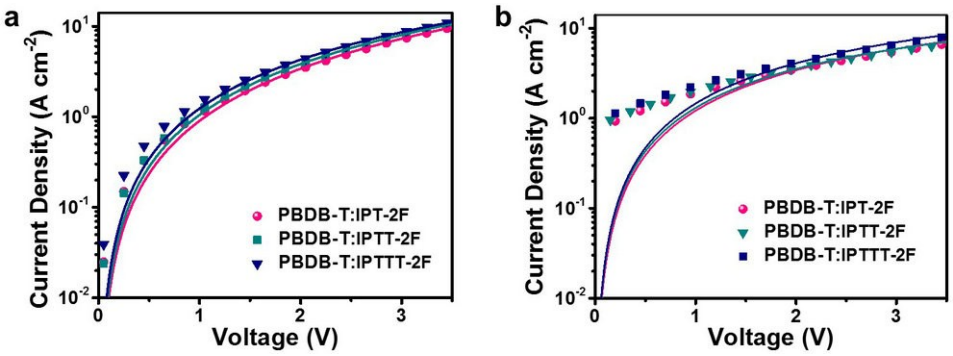

Fig. S33 a) Hole mobility plots from SCLC measurement. b) Electron mobility plots from SCLC measurement.

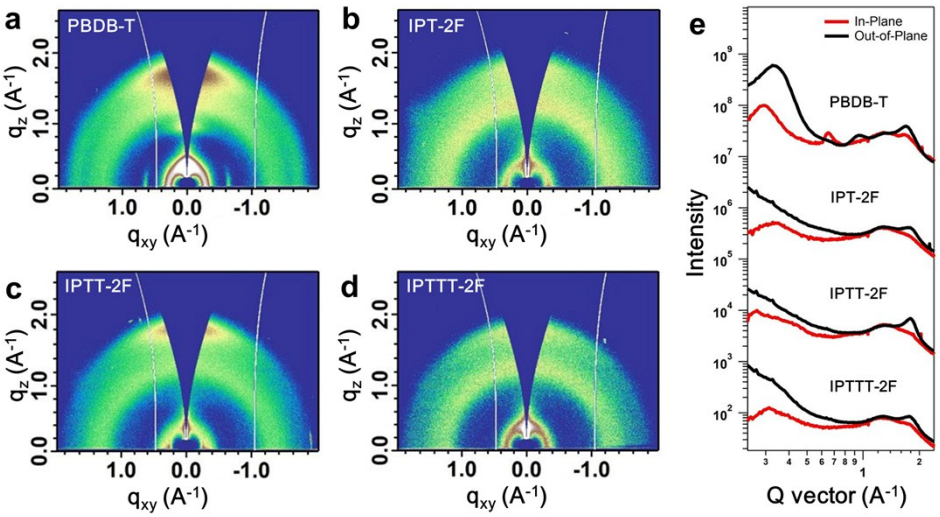

Fig. S34 (a-d) GIWAXS patterns of PBDB-T, IPT-2F, IPTT-2F, and IPTTT-2F neat films. (e) Corresponding line cuts of the GIWAXS images.

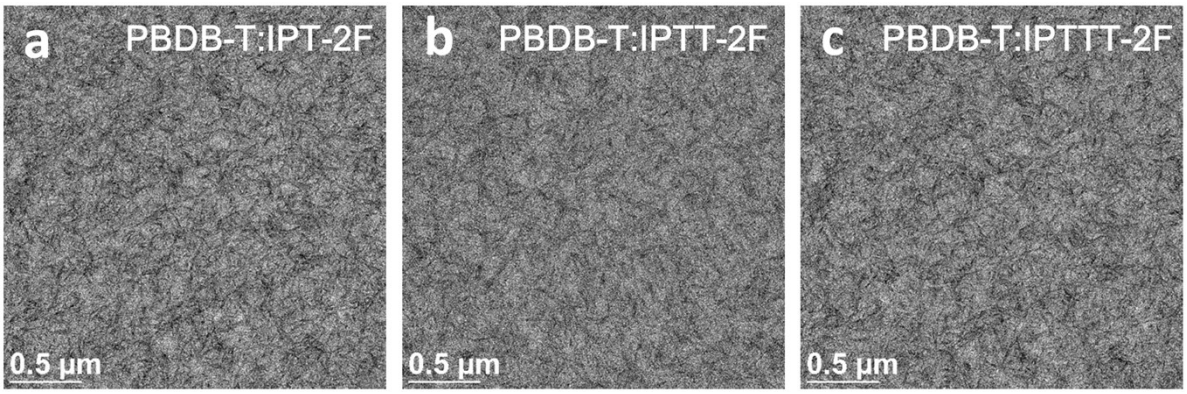

Fig. S35 TEM images of (a) IPT-2F, (b) IPTT-2F, and (c) IPTTT-2F based blend films.

References

[1] J. Sun, X. Ma, Z. Zhang, J. Yu, J. Zhou, X. Yin, L. Yang, R. Geng, R. Zhu, F. Zhang, W. Tang, *Adv. Mater.* **2018**, *30*, 1707150.

[2] K. Kawabata, M. Takeguchi, H. Goto, *Macromolecules* **2013**, *46*, 2078-2091.

[3] L. Zhang, L. Tan, W. Hu, Z. Wang, *J. Mater. Chem.* **2009**, *19*, 8216-8222.

[4] J. Song, C. Li, L. Ye, C. Koh, Y. Cai, D. Wei, H. Y. Woo, Y. Sun, *J. Mater. Chem. A* **2018**, *6*, 18847-18852.

[5] C. Li, J. Song, L. Ye, C. Koh, K. Weng, H. Fu, Y. Cai, Y. Xie, D. Wei, H. Y. Woo, Y. Sun, *Sol. RRL* **2019**, *3*, 1800246.

[6] S. Dai, F. Zhao, Q. Zhang, T.-K. Lau, T. Li, K. Liu, Q. Ling, C. Wang, X. Lu, W. You, X. Zhan, *J. Am. Chem. Soc.* **2017**, *139*, 1336-1343.

[7] W. Wang, C. Yan, T.-K. Lau, J. Wang, K. Liu, Y. Fan, X. Lu, X. Zhan, *Adv. Mater.* **2017**, *29*, 1701308.

[8] B. Gao, H. Yao, J. Hou, R. Yu, L. Hong, Y. Xu, J. Hou, *J. Mater. Chem. A* **2018**, *6*, 23644-23649.

[9] W. Gao, T. Liu, J. Li, Y. Xiao, G. Zhang, Y. Chen, C. Zhong, X. Lu, H. Yan, C. Yang, *J. Mater. Chem. A* **2019**, *7*, 11053-11061.

[10] J. Zhang, W. Liu, S. Chen, S. Xu, C. Yang, X. Zhu, *J. Mater. Chem. A* **2018**, *6*, 22519-22525.

[11] W. Gao, Q. An, C. Zhong, Z. Luo, R. Ming, M. Zhang, Y. Zou, F. Liu, F. Zhang, C. Yang, *Chem. Sci.* **2018**, *9*, 8142-8149.

[12] W. Gao, T. Liu, C. Zhong, G. Zhang, Y. Zhang, R. Ming, L. Zhang, J. Xin, K. Wu, Y. Guo, W. Ma, H. Yan, Y. Liu, C. Yang, *ACS Energy Lett.* **2018**, *3*, 1760-1768.

[13] W. Gao, F. Wu, T. Liu, G. Zhang, Z. Chen, C. Zhong, L. Zhu, F. Liu, H. Yan, C. Yang, *J. Mater. Chem. A* **2019**, *7*, 2412-2420.

[14] C. Li, T. Xia, J. Song, H. Fu, H. S. Ryu, K. Weng, L. Ye, H. Y. Woo, Y. Sun, *J. Mater. Chem. A* **2019**, *7*, 1435-1441.

[15] M. Li, Y. Zhou, J. Zhang, J. Song, Z. Bo, *J. Mater. Chem. A* **2019**, *7*, 8889-8896.

[16] L. Ye, Y. Xie, Y. Xiao, J. Song, C. Li, H. Fu, K. Weng, X. Lu, S. Tan, Y. Sun, *J. Mater. Chem. A* **2019**, *7*, 8055-8060.

[17] W. Gao, M. Zhang, T. Liu, R. Ming, Q. An, K. Wu, D. Xie, Z. Luo, C. Zhong, F. Liu, F. Zhang, H. Yan, C. Yang, *Adv. Mater.* **2018**, *30*, 1800052.

[18] Feng, C. E. Zhang, Y. Liu, Z. Bi, Z. Zhang, X. Xu, W. Ma, Z. Bo, *Adv. Mater.* **2017**, *29*, 1703527.

[19] C. Li, Y. Xie, B. Fan, G. Han, Y. Yi, Y. Sun, *J. Mater. Chem. C* **2018**, *6*, 4873-4877.

[20] C. Li, J. Song, Y. Cai, G. Han, W. Zheng, Y. Yi, H. S. Ryu, H. Y. Woo, Y. Sun, *J. Energy Chem.* **2020**, *40*, 144-150.

[21] S. Feng, C. e. Zhang, Z. Bi, Y. Liu, P. Jiang, S. Ming, X. Xu, W. Ma, Z. Bo, *ACS Appl. Mater. Interfaces* **2019**, *11*, 3098.

[22] W. Zhai, A. Tang, B. Xiao, X. Wang, F. Chen, E. Zhou, *Sci. Bull.* **2018**, *63*, 845-852.

[23] Z. Luo, G. Li, K. Wu, Z.-G. Zhang, X. Chen, B. Qiu, L. Xue, Y. Li, C. Yang, *Org. Electron.* **2018**, *62*, 82-88.

[24] Y. Zhao, Z. Luo, G. Li, J. Luo, Z. G. Zhang, Y. Li, C. Yang, *Chem. Commun.* **2018**, *54*, 9801-9804.

[25] R. Geng, X. Song, H. Feng, J. Yu, M. Zhang, N. Gasparini, Z. Zhang, F. Liu, D. Baran, W. Tang, *ACS Energy Lett.* **2019**, *4*, 763-770.

[26] C. Huang, X. Liao, K. Gao, L. Zuo, F. Lin, X. Shi, C.-Z. Li, H. Liu, X. Li, F. Liu, Y. Chen, H. Chen, A. K. Y. Jen, *Chem. Mater.* **2018**, *30*, 5429-5434.

[27] H. Feng, X. Song, M. Zhang, J. Yu, Z. Zhang, R. Geng, L. Yang, F. Liu, D. Baran, W. Tang, *Mater. Chem. Front.* **2019**, *3*, 702-708.